UNIVERSITÀ DEGLI STUDI DI PADOVA
DIPARTIMENTO DI INGEGNERIA INDUSTRIALE
CORSO DI LAUREA IN INGEGNERIA CHIMICA E DEI PROCESSI INDUSTRIALI

Tesi di Laurea Magistrale in
Ingegneria Chimica e dei Processi Industriali

Risk analysis of industrial plant submitted to major accident due to natural events

Relatore: Prof. Ing. Giuseppe Maschio
Correlatore: Ing. Chiara Vianello

Laureanda: BEATRICE POZZI

ANNO ACCADEMICO 2016 – 2017

Riassunto

Lo scopo di questo elaborato è quello di proporre un metodo che permetta il calcolo del rischio di incidenti rilevanti indotti da eventi naturali in impianti fissi. L'analisi del rischio convenzionale non è sufficiente per adempiere questo compito. Per questo motivo si sono utilizzati due metodi alternativi, che sono stati applicati in due diverse località: Porto Marghera (VE), in cui c'è la sede della bio-raffineria di Eni, e Priolo Gargallo (SR). La scelta è stata dettata dalle diverse caratteristiche territoriali delle due aree, in modo da poter fare dei confronti.

Partendo dall'albero dei guasti di un serbatoio di stoccaggio di green diesel dell'impianto Eni di Porto Marghera, si è applicato il metodo DyPASI. Tale tecnica è costituita da 5 fasi: la fase 0 consente di effettuare il "punto della situazione" realizzando il bow-tie; la fase 1 richiede la raccolta di informazioni attraverso motori di ricerca contenenti dati su incidenti o mancati incidenti e, per valutare se tali informazioni possono essere coerenti con il contesto in cui opera l'impianto, è effettuata un'analisi sulla vulnerabilità del territorio; la fase 2 consente di fare una lista di priorità degli eventi raccolti durante la fase precedente affinché si possa valutare se sia effettivamente necessario per esse condurre un'ulteriore analisi; la fase 3 è l'identificazione effettiva degli scenari atipici; la fase 4 è l'identificazione delle barriere di sicurezza.

L'applicazione della DyPASI ha consentito di identificare nuove cause e nuovi scenari per il top-event su cui lo studio si è focalizzato, dimostrando in tal modo i vantaggi dell'integrazione di questa tecnica innovativa con le tecniche convenzionali.

Una volta ottenuto il bow-tie aggiornato, si è passati al calcolo della frequenza di rottura del top-event. A questo punto si è dovuto scegliere se usare un approccio deterministico o probabilistico. Avendo a che fare anche con frequenze di rottura a causa di terremoti, si è preferito l'approccio probabilistico. Si sono quindi dovute convertire le frequenze di rottura dei componenti meccanici mediante l'utilizzo di una funzione esponenziale. In questo modo è possibile ottenere le distribuzioni di probabilità di guasto per l'apparato meccanico coinvolto, grazie all'uso di un programma di calcolo. Allo stesso modo sono state ottenute le distribuzioni di probabilità di guasto dovute a piogge violente.

Questi dati sono, dunque, compatibili con quelli che è possibile ottenere dall'analisi sismica: attraverso la matrice di distribuzione dei terremoti, al vettore frequenza e alle curve di fragilità dei materiali si ottiene la probabilità di guasto legata all'evento sismico.

I contributi dovuti ad eventi naturali vengono sommati e quindi moltiplicati al contributo dovuto al guasto dell'apparato meccanico così da ottenere un dato generale, che tenga conto

di tutte le possibili origini del rischio (meccaniche e naturali) in ottemperanza alla “Direttiva Seveso III”.

Risultati diversi si ottengono nelle due zone: dall’analisi di vulnerabilità infatti emerge che l’area di Porto Marghera è soggetta ad inondazioni ed è una zona a basso rischio sismico, sebbene sia da prestare attenzione sul fatto che sia circondata da zone sismiche (Friuli, Emilia). D’altra parte Priolo Gargallo è un’area ad elevato rischio sismico. Per cui gli alberi dei guasti e le relative frequenze saranno differenti. Inoltre, i calcoli sono stati fatti sia nel caso di serbatoi ancorati che non ancorati e i risultati ottenuti evidenziano che per le zone sismiche si debbano prendere in considerazione sistemi di isolamento sismico.

Abstract

The aim of this study is to develop a methodology that allow the calculation of the risk of relevant accident due to natural events in industrial plants. Conventional risk assessment is insufficient to perform this work. For this reason, two new methodologies are used and they have been applied in two different locations: Porto Marghera (VE) and Priolo Gargallo (SR). These choices are not casual, they have different territorial characteristics.

DyPASI is the first approach to be used, it's composed of five steps and at the end of the analysis the new bow-tie is obtained and it considers also natural events. From the vulnerability analysis of the two locations, the result is that Porto Marghera is affected by heavy rainfall and earthquakes, while Priolo Gargallo is a highly seismic area.

The next step is the calculation of the failure frequency of the top-event. First of all, it is decided to use the probabilistic approach; mechanical failure frequency and heavy rainfall failure frequency are converted in probabilistic failure distribution by means of exponential function.

In this way, these data are compatible with the ones that is possible to obtain performing a seismic analysis: through the matrix of distribution of earthquakes, the frequency vector and the fragility curves of the equipment it is possible to obtain the probability of failure due to earthquakes. The global result is obtained summing the contributions of natural events and then multiplying them with the mechanical contribution.

Thus, all possible sources of risk (due to mechanical failure and natural events) are taken into account in compliance with the "Seveso III Directive".

Contents

Introduction

Nowadays, the risk assessment of chemical plants is considered a key parameter in terms of investment opportunity. In particular, safety perception in public opinion is an important factor that can determine the acceptance of a plant by surrounding inhabitants.
In addition, climate changes caused an increasing frequency of severe natural events and the damage of process equipment due to the impact of natural events is known to have triggered a number of severe accidents in the chemical and process industry due to the loss of containment of hazardous substances.
For these reasons, it's important to carry out a risk analysis, which is the result of a multi-disciplinary investigation, in order to consider also natural events.
Thus, conventional risk analysis is left out and two new methods are considered: DyPASI technique is used to develop the qualitative risk assessment, while for the quantitative risk assessment the probabilistic fault tree analysis is performed.

This thesis is composed of six chapters.
In Chapter 1, natural disasters, such as earthquakes and floods, are described and it's discussed how it is possible to evaluate seismic and flooding risk for a chemical equipment.
Also the regulatory framework is briefly discussed in Chapter 1 (concerning safety in chemical plants), in particular Seveso Directive and its modification are described. In 2012, the "Seveso III Directive" was promulgated and it considers, for the first time, domino effect due to natural events such as flooding and earthquakes. Seismic events are a characteristic of Italy: in fact, there are several seismic areas and almost all the peninsula is submitted to this risk. In addition, in recent years, some regions of Italy are characterized by radicalization of the clime, especially due to heavy rainfalls.
Chapter 2 deals with conventional risk assessment procedure: the first step is the Hazard Identification, which can be carried out with several approaches, that can be qualitative, or semi-quantitative. Among the qualitative approaches there are historical analysis of incidents and accidents, check lists and the "what if" analysis; while semi-quantitative approaches are: HazOp (Hazard and Operability study), FMEA (Failure Mode and Effect Analysis) and FMECA (Failure Mode, Effect and Criticality Analysis). Then the quantitative hazard analysis, with the fault and event tree, is described.
In Chapter 3 limitations of the classical risk analysis are highlighted and then DyPASI technique and probabilistic fault tree are introduced as solutions to cope with these limits.

In Chapter 4, the locations of case studies are described. In fact, location can determine the final value of the risk analysis. It's carried out the vulnerability analysis of the two locations and then it's applied the DyPASI technique in order to obtain the updated bow-tie.
In Chapter 5 it's described the procedure used to develop the fault tree analysis and it's also explained the numeric code applied.
Chapter 6 shows the results of risk analysis obtained using the procedure described in Chapter 5. Simulations are performed for anchored and unanchored tank, thus it's possible to compare conclusive results and make some considerations.
The methodology used in this work allows to give a first try in risk analysis as the "Seveso III Directive" asks.

Chapter 1

Interaction between natural events and industrial structures

Natural disasters, such as earthquakes and floods, can impact industrial installations that process or store hazardous materials, potentially causing major accidents with fires, explosions or toxic releases.
A literature analysis has shown that none of the European countries have specific risk and emergency management programs in place which contemplate explicitly the occurrence of natural disaster interacting with industrial installations.
On the other hand, 'Seveso Directive III' in 2012 emphasized preparation of emergency plans, involving the public in consultation and decision making and including identification and accidental risks analysis and prevention methods also for natural causes, such as earthquakes and floods. To deal with these procedures a multi-disciplinary effort is needed.

1.1 Natural-Technological accidents

Natural catastrophic events may affect the integrity of industrial structures (equipment, auxiliary system, instrumentation, structural support, utilities). Therefore, loss of energy or mass or, more generally, both mass and energy from the containment system is likely to occur. If industrial facilities store large amount of hazardous materials, accidental scenarios as fire, explosion, or toxic dispersion may be triggered, thus possibly involving working people within the installation and/or population living in the close surrounding or in the urban area where the industrial installation is located. Accidents of this type are commonly referred to as Natural-Technological (Na-tech) accidents.
To consider every possible external event, that is an event whose cause is external to all systems used in normal operation, a diligent study of geologic, seismologic, hydrologic, and meteorological characteristics of the site region as well as present and designed industrial activities near the plant should be conducted. An example of list of natural external events is shown in Table 1.1. Each external event has to be reviewed to judge whether it deserves further studies.
The knowledge of the plant and its design basis are used to screen out from the list all the hazards that, reasonably, have a negligible contribution to risk of the plant.

Table 1.1. *List of natural external events*

Seismic activity	Intense precipitation
Coastal erosion	Low winter temperature
External flooding	External winds and tornadoes
Fire	River diversion
Sandstorm	Fog
Forest fire	Snow
Frost	Hail
Soil shrink-swell consolidation	High summer consolidation
Hurricane	Storm surge
Ice cover	Tsunami
Internal flooding	Landslide
Volcanic activity	Lightning
High lake or river water level	Waves

A particular hazard can be screened out if:

- The event has a damage potential equal or lower than the specific events for which the plan has been designed. This required an evaluation of plant design bases in order to estimate performance against a specific external event. This screening criterion is not applicable to events like earthquakes, floods, and extreme winds since their hazard intensities could conceivably exceed the plant design bases.
- The event has a significantly lower mean frequency of occurrence than other events with similar uncertainties and could not result in worse consequences than those events.
- The hazard cannot take place close enough to the plant.
- The event is included in the definition or consequences of other events. For example, storm surge is included in external flooding.

1.2 Earthquakes

The interaction between earthquakes and industrial equipment can result in extensive damage when hazardous processes are involved (Na-Tech risks). Consequently, industrial risk assessment should consider the consequences and the likelihood of occurrence of accidental scenarios triggered by such natural events. To this regard, it is worth noting that Na-Tech procedures need multi-disciplinary effort: definition of probability of occurrence of earthquake intensity (i.e. Probabilistic Seismic Hazard Analysis or PSHA), structural analysis of equipment under seismic actions, forecast of specific response of industrial processes due to the given structural damage of equipment, are indeed all necessary steps to be added to the classical methodologies for the re-composition of industrial risks.

However, this is not the unique available option. An interesting approach to Na-Tech risk mitigation is represented by seismic early warning systems (EWS); EWS is a set of actions that can be taken from the moment when a seismic event is detected with significant reliability to the moment the earthquake strikes in a given location.

1.2.1 Earthquake characterization and prediction

In order to understand how to mitigate and to cope with earthquakes, it's important to know how they "work". Ground motions are generated by seismic waves radiating from the earthquake focus to the site. Their intensities have to be related to the earthquake source, to the path for the seismic waves from the source to site, and to the specific geomorphologic characteristics of the site where the Na-Tech is performed. Many random features of earthquakes, including energy, frequency contents, and phases affect the actions applied to the structures and thus their structural response.

Earthquake signals carry several uncertainties and it is not even a trivial task to define a univocally determined "intensity" of earthquake, thus allowing comparison of records. However, geophysicists and structural engineers use to classify earthquakes based on two classes of parameters such as "ground parameters" and "structural dynamic affecting factors". The choice of these intensity parameters is important since they summarise all the random features of earthquakes.

Ground parameters refer to the intensity measures (IM) characterising the ground motion: PGA or alternatively peak ground velocity (PGV) and response spectra (RS) at the site location of the component.

Structural affecting factors usually refer to the dynamic amplification induced on a single degree of freedom system with the same period of the analysed structure (first mode spectral acceleration), although experimental investigations have shown that different parameters are needed if the effects of earthquake on structures would be accurately reproduced by structural analysis. For instance, in seismic analysis of piping system PGV is commonly used, whereas PGA is more useful when steel storage tanks are under investigation.

Currently, the problem of definition of effective and reliable predictors for inelastic seismic behaviour of structures is one of the main topics of earthquake engineering. However, empirical vulnerability analyses are often carried out in terms of peak ground acceleration, mainly because it is relatively easy to infer by earthquake intensity conversion. Furthermore, extensive historical databases on structural damages are usually defined by PGA; and transformation from typical earthquake magnitude (e.g. Modified Mercalli or Richter scale) to this variable is generally accepted.

For the aims of early warning system, additional information is useful on the time of arrival of seismic wave from the focus point. In the framework of industrial risk analysis only two types are of primary interest: P (primary) waves, which travel faster and are the first to be recorded, and S (secondary) waves, that together with other type of waves (surface waves) produce most of damages and destruction. P waves can travel through any medium, whereas S waves can only travel through solids. Surface waves are slower than P and S waves and can only travel on the surface of the earth.

The speed of a seismic wave is not constant but is dependent upon many factors. Speed changes mostly with depth and rock type. P waves travel between 6 and 13 km/s. S waves are slower and travel between 3.5 and 7.5 km/s. Hence, the distance of seismic recording station to the earthquake epicentre can be known by using the times of travel of the S and P waves.

Figure 1.1 shows the time of arrival of seismic P and S waves, and their time difference, for any location at distance from focus point.

Data reported in Figure 1.1 can be usefully adopted for early warning issues. In fact, several seconds may elapse between the arrival of the first P wave at the monitoring station and the arrival of the damaging S and surface waves and this time interval increases with the distance from the focus of the earthquake.

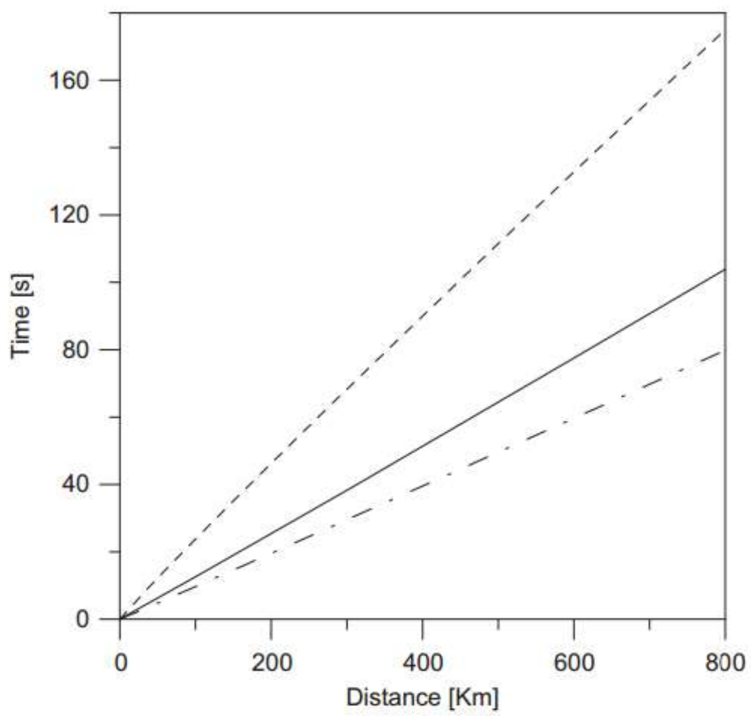

Figure 1.1. *Time of arrival of seismic waves with respect to distance of earthquake focus point. ---: S waves; ——: P waves; – · –: (S–P) waves.*

1.3 Fragility analysis for industrial equipment

Behaviour of structures and components under load induced by external hazard event, like earthquakes, is relevant and must be assessed to evaluate probabilities of faults and malfunctioning. This process is based generally on structural analysis and relates intensity measures of a given loads to effects on the structures. However, typical industrial accidental scenarios in the process industry (explosion, fire, toxic dispersion) depend basically on the total amount of released dangerous substances.

Accordingly, seismic vulnerability of equipment should be given either in terms of structural damage or in terms of following content release. Therefore, in the mainframe of industrial risk analysis, existing database concerning post-earthquake, structural damage observations for industrial equipment must be optimized and reorganized in terms of new risk categories. Quite clearly, because of incomplete descriptions of the actual damage to equipment into empirical database considered, the definition of damage state or risk state is somehow depending on technical judgment other than the described consequences suffered by industrial components.

The structural damage produced by seismic action on equipment may be referred as ‘‘damage state’’ (DS), in total analogy with definition, which has been extensively used to evaluate from the structural perspective the economical effort needed to repair and restore the tank structures. According to HAZUS damage classification, DS values may rank from DS1 to DS5. No damage is identified as DS1, slight damage to structures as DS2, moderate damage as DS3, extensive damage as DS4 and the total collapse of structure as DS5.

On the other hand, as already mentioned, all typical large-scale accidental scenarios in the process industry (e.g. vapor cloud explosion, gas explosion, flash fire, jet fire, tank and pool fire, toxic dispersion) depend on the total amount of released dangerous substance. Hence, seismic vulnerability of large-scale industrial equipment should be expressed in terms of content release, integrating and extending the classical concept of exceedance probability of any given structural state. Eventually, a risk state RS can be defined regarding the loss of content from each containment system or equipment.

For both DS and RS, probability of occurrence can be assessed by means of fragility curves F expressed in terms of log-normal cumulative distribution (cdf), characterized by mean μ and standard deviation β for any DS or RS state:

$$F_{DS} = cdf(\mu_{DS}, \beta_{DS}, lnPGA), F_{RS} = cdf(\mu_{RS}, \beta_{RS}, lnPGA) \quad (1.1)$$

In Equation (1.1), PGA is the realization of the seismic intensity that triggers the failure corresponding to the damage or risk state of interest.

Due to the lack and uncertainties on observations, large scatter of data for values of probability close to zero is observed.

Hence for the definition of PGA threshold values for any risk or damage state, a Probit analysis has been usefully carried out.

The Probit value Y allows the linearization of sigma-shaped statistical function and it is characterized by two constants k_1 and k_2:

$$Y = k_1 + k_2 \ln(PGA) \quad \forall DS, RS \;\; PGA \; given \; as \; a \; fraction \; of \; g \qquad (1.2)$$

The variable Y is then related to probability (fragility) by means of a simple integration.
Fragilities F can be evaluated by databases and observational analysis if considering all possible failure probability (included in the DS definition), given the seismic intensity IM expressed in terms of peak ground acceleration:

$$F_{DS} = \bigcup_{i=1}^{\infty} Failure \; \cap IM \qquad (1.3)$$

If any failure cannot take place for a given IM, if another value has already led the system to the same failure, events in the previous equation are mutually exclusive and union of events probability is given by the sum of the probabilities.

1.3.1 Atmospheric storage tanks

Dynamic behaviour of atmospheric storage tanks when subjected to earthquake is dominated by complex fluid–structure interaction phenomena. However, two predominant modes of vibration can be identified. The first one can be schematically related to a fraction of the total mass that behaves as rigid and moves together with the tank structure (impulsive mass), the other can be related to liquid sloshing (convective mass).
Seismic actions trigger global overturning moments and base shear induced by horizontal forces of inertia. Overturning moment causes an increase of the vertical stress in the tank wall and even uplift of the base plate, while base shear can lead to relative displacements between the base plate and the foundation.
Failure modes reflect these specific aspects of the seismic demand on the structure and depend basically upon the type of interface at the tank base. Mechanical devices are used to ensure an effective connection between the base plate and the foundation (unanchored or anchored). When unanchored tanks are of concern, friction at the base is able to ensure the needed stability of the structure under environmental actions, i.e. wind, but can be ineffective when strong ground motions take place and large relative displacements can be generated.
On the other hand, tank sliding reduces the maximum acceleration suffered by the equipment. In the case of relatively small frictional factor may result in large relative displacements and consequently large deformations and even failure of piping and connections may occur.
Another damage mechanism is represented by the partial uplift of the base plate. This phenomenon reduces the hydrodynamic forces in the tank, but can increases significantly axial compressive stresses of the tank wall. This is the reason why a characteristic buckling of the wall (elephant foot bucking—EFB) occurs. EFB is normally observed when large diameter tanks with height to radius (H/R) ratios in the range 2–3 are considered.

A different buckling mode, known as diamond shape buckling (DSB), is conversely generated in taller tanks, i.e. H/R about 4. It is worth noting that the EFB is related to an elastic–plastic state of stress, while DSB is a purely elastic buckling. Depending on the type of tank and its functional and structural detailing, additional structural damages can be expected, namely collapse of support columns for fixed roof tanks, foundation collapse due to soil liquefaction, splitting and leakage associated only with bolted and riveted tanks.

Liquid sloshing during earthquake action produces several damages by fluid–structure interaction phenomena and can result as the main cause of equipment damage for full or nearly full tanks.

Historical analysis and assessment of seismic damages of storage tanks have demonstrated that only full (or near full) tanks experienced catastrophic failures. Low H/R tanks only suffered cracks in conical roof connection, or damage by floating panel sinking.

As EFB is concerned, it is not frequent in the case of unanchored tanks with $H/R<0.8$, that they can suffer conversely base plate and/or shell connection failures resulting in content spillage.

A full stress analysis is certainly the most accurate way to design and to evaluate the risk of steel tanks under earthquake loads. This approach leads to the direct computation of the interaction between shell deformations and content motion during earthquakes. For base constrained and rigid tanks (anchored), a complete seismic analysis requires solution of Laplace’s equation for the motion of the contained liquid, in order to obtain the total pressure history on the tank shell during earthquakes. When flexible tanks are considered, a structural deformation term must be also added to take account of the “impulsive” and “convective” contributions.

Actually, the quantitative assessment of risk within a complex industrial installation needs the analysis of a large number of components. Hence, for sake of simplification, statistical and empirical tools derived from post-accident analysis are useful to define easy to manage and general vulnerability functions.

DS values have been reviewed as three levels of intensity of loss of containment, defined as RS (risk state): no loss—RS1, moderate loss—RS2, extensive loss of containment—RS3.

Tables 1.2 and 1.3, taken from Salzano *et al.* (2003), report the coefficients μ and β of cumulative log-normal distribution for the probability of occurrence of RS for anchored and unanchored storage tanks respectively, and the correspondent coefficients k_1 and k_2 for Probit function, depending on PGA expressed in terms of g fractions (acceleration of gravity). Threshold values for the PGA for each damage or risk state (PGA_k) are also reported for the sake of early warning systems issues.

Table 1.2. *Seismic fragility and Probit coefficients for anchored atmospheric steel tanks.*

RS	Fill Level	μ(g)	β(g)	k_1	k_2	PGA_k(g)
≥2	near full	0.30	0.60	7.01	1.67	0.074
3	near full	1.25	0.65	4.66	1.54	0.275
≥2	≥50%	0.71	0.80	5.43	1.25	0.110
3	≥50%	3.72	0.80	3.36	1.25	0.577

Table 1.3. *Seismic fragility and Probit coefficients for unanchored atmospheric steel tanks.*

RS	Fill Level	μ(g)	β(g)	k_1	k_2	PGA_k(g)
≥2	near full	0.15	0.70	7.71	1.43	0.029
3	near full	0.68	0.75	5.51	1.34	0.118
≥2	≥50%	Nd				
3	≥50%	1.06	0.80	4.93	1.25	0.164

The term “Nd” in table 1.3 means that data for statistical analysis are insufficient or not available. The terms μ, β, $k_1$and k_2, reported in Table 1.2 and 1.3, are, respectively, the cumulative distribution function parameters and the Probit coefficients (Equations (1.1) and (1.2), respectively). PGA_k is the threshold value for the risk state.
Results reported in Tables 1.2 and 1.3 can be used as basic information to predict accidental scenarios as fires (pool fire, flash fire, tank fire), explosions (in the case of formation large vapour cloud) or, when toxic vapour are formed, for the dispersion analysis.

1.4 Floods

The increasing frequency of severe natural events caused by climate changes raised a concern about the possible interference of these external hazards with industrial activities. However, presently scarce attention is devoted to the assessment of the risk related to accidents triggered by natural events, as well as to the prevention and to the consequence assessment of the specific accidental scenarios.
The selection and characterization of reference flood events may be based on the return time and on two severity parameters of the flood: the maximum water depth expected at the site and the flood energy, usually expressed as the maximum expected water speed. Even if these parameters are usually not reported in general flood hazard assessment studies, they may become available from specific analyses carried out on the site. Again, it should be remarked that by no means these parameters may be sufficient to fully characterize the flood hazard of a

site, but they are suitable to characterize the severity of the reference events in the present approach.

The following step in the evaluation of industrial accidents triggered by floods is the identification of the reference incidental scenarios due to the release of hazardous materials following the flood. In order to identify the reference scenarios that need to be considered, three parameters should be analysed:

- the hazardous properties of the substances;
- the hold-up of the equipment, which influences the quantity of substance released;
- the expected type of structural damage.

Antonioni *et al.* (2009) state that storage tanks are the equipment items more frequently affected by loss of containment triggered by flood.

In the case of floods, besides substances having "conventional" hazards considered in off-site consequence assessment of industrial accidents (flammability or toxicity), the analysis should be extended to substances reacting with water and/or developing flammable/toxic gases in contact with water. Indeed, it must be remarked that besides conventional release scenarios (fires, explosions and toxic clouds), floods may cause two further critical events: significant environmental contamination due to water pollution, and release of toxic gases and flammable vapours generated by reactions of chemicals with water.

Also in the case of floods, reference damage states were defined to characterize equipment damage. Damage states were defined on the basis of equipment classification based on structural characteristics. The equipment categories defined are the following: (i) cylindrical vertical vessels having diameter to height (D/H) ratio higher than 1 (atmospheric); (ii) cylindrical vertical vessels having D/H<1 (atmospheric and pressurized); (iii) cylindrical horizontal vessels (atmospheric and pressurized).

Three possible modalities of water impact were assumed and were associated to credible typologies and extents of structural damage: slow submersion (water velocity negligible), low-speed wave (water velocity below 1 m/s), and high-speed wave (water velocity higher than 1 m/s). Also in the case of floods, three classes of releases were considered for storage and process equipment, as well as for piping: R1 defines the instantaneous release of the complete inventory (in less than 2 min) following severe structural damage; R2 the continuous release of the complete inventory (in more than 10 min); R3 the continuous release from a hole having an equivalent diameter of 10 mm. This classification is the opposite of the one made in the case of earthquake damage.

The accidental scenarios that are expected to follow the releases were identified by the event tree technique, taking into account the possible scenarios deriving from substances reacting with water.

In the case of floods, no simplified equipment damage models are available in the literature. Very limited data are available in the open literature to analyse in detail the damage caused by floods to industrial equipment. The information about past accidents recorded in industrial accident databases is usually not sufficiently detailed, in particular with respect to the description of the structural damage of equipment caused by the flood. Furthermore, in several reports available for past accidents, the flood severity parameters are not recorded.

1.5 Seveso directive

The chief piece of legislation in Europe relating to the prevention and control of chemical accidents is the ‘Seveso Directive’, which has its roots in the aftermath of the industrial accident that occurred in Italy in the mid-70s.

In 1976, an explosion in a small chemical plant led to the release of a toxic cloud containing 2,3,7,8-tetrachlorodibenzo-p-dioxin (TCDD) that contaminated a densely-populated area of about 10 square miles between Milan and Lake Como. The cloud was concentrated around the municipality of Seveso, located downwind from the plant.

The accident led to the adoption in 1982 of the European Union Directive 82/501/EC relating to major chemical accidents, which came to be known as the ‘Seveso Directive’. The legislation aims to prevent the occurrence of major accidents at sites that store, produce or make use of dangerous substances in sufficient quantities to constitute a serious health, safety and/or environmental risk, and to limit the consequences for people and the environment in the event of such an accident.

Within the European Union (EU), in ‘Seveso I’ regulatory environment for the chemical process industry (EC, 1982), major accidents have been defined as “sudden, unexpected, unplanned events, resulting from uncontrolled developments during an industrial activity, which actually or potentially cause serious immediate or delayed adverse effects (death, injuries, poisoning or hospitalisation) to a number of people inside and/or outside the installation”, (EC, 1982, 1988). ‘Seveso I’ was later amended in view of the lessons learned from later accidents such as Bhopal or Toulouse resulting into ‘Seveso II’ (Directive 96/82/EC).

The ‘Seveso II Directive’ which replaces and strengthens ‘Seveso I’, includes now a concise and unequivocal definition of what constitutes a “major accident” based on precise quantitative threshold criteria which will most probably result in an overall lowering of the criteria for notification. In addition, it introduces the concept of safety management system and it requires also attention for domino effects to neighbouring plants, for land use planning, and for care in plant modifications.

The legislation applies to establishments where various dangerous substances are present in quantities equal to, or above, a given threshold, while the legislation does not apply to certain activities and installations, such as military establishments, land-fills, hazards caused by ionising radiation, and the transport of dangerous substances outside the establishments.

In 2012 ‘Seveso III’ was adopted considering, amongst others, the changes in the Union legislation on the classification of chemicals and increased rights for citizens to access information and justice. It replaces the previous ‘Seveso II Directive’.
The Directive now applies to more than 10 000 industrial establishments in the European Union where dangerous substances are used or stored in large quantities, mainly in the chemical, petrochemical, logistics and metal refining sectors.
There’s also another statement added in the Annex II of ‘Seveso III Directive’ that is worth noting because it’s significant for the aim of this thesis. It says that a detailed description of the possible major-accident scenarios and their probability or the conditions under which they occur is needed including also natural causes, for example earthquakes or floods.
Thus, it’s important to understand how to consider these natural events in the risk assessment procedure and this is the main topic of Chapter 3.

Chapter 2

Conventional risk assessment

The topic of this chapter is the description of the classical risk assessment procedure, which is composed by several steps. But first it's highlighted the distinction between hazard and risk and their definitions, since they are important features when dealing with industrial risk assessment.

2.1 Risk and hazard

Comprehensive and complete identification and assessment of potential hazards and risks in the process industry are of primary importance. First of all, it's meaningful to define the concepts of hazard and risk. A hazard is "any property or intrinsic quality of a specific factor that has the potentiality to cause damages", whereas a risk is "the probability to reach the potential threshold of damage in the conditions of use and exposition to a specific factor or agent or both of them", according respectively to the D. Lgs. of 9 April 2008, n. 81, art. 2, paragraph 1, letter r and s.

The risk (R) is defined as the product of the occurrence frequency (*f*) and the magnitude of consequences (M):

$$R = f \cdot M$$

Based on this equation, a risk could be high when events are frequent but with low consequences, or when there are rare events with catastrophic consequences. This distinction is important dealing with risk reducing measures because it's possible to undertake mitigation measures to minimize the probability of the undesired event, or prevention measures to prevent the consequences of the event.

2.2 Risk assessment procedure

The conventional risk assessment procedure is reported in Figure 2.1, where it's easy to see all the steps involved in the analysis.

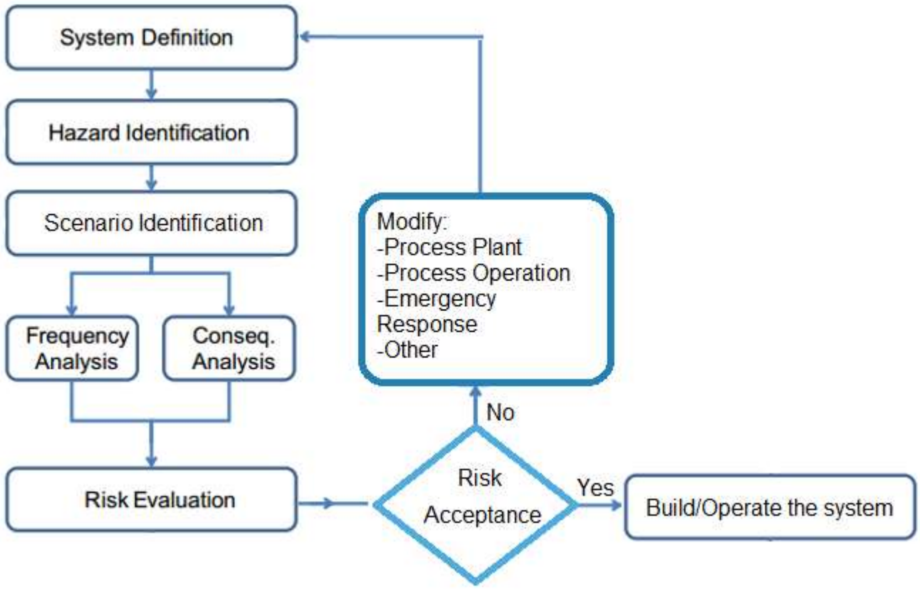

Figure 2.1. *Hazard identification and Risk assessment procedure*

2.2.1. Hazard Identification

Once the system description is given, the first step of the risk assessment procedure is the Hazard Identification (HazId), which is a fundamental stage, that requires to know the process, the plant equipment, and raw materials and products involved. It can be carried out with several approaches, that can be qualitative, or semi-quantitative.

2.2.1.1 The qualitative methods

Among the qualitative methods there are: the historical analysis of incidents and accidents, check lists and the "what if" analysis.
The historical analysis consists in the investigation and collection of all the accidents that are similar to the one supposed (similar plants, similar materials/products, similar climatic conditions, etc.). Data banks are essential when dealing with this method.
The check list is intended to promote thought; to raise questions such as: is it needed, what are the alternatives, has provision been made for, checked for, has it been provided?
Some companies make use of safety indices as a tool for assessing the relative risk of a new process or plant. The most widely used safety index is the Dow Fire and Explosion Index, developed by the Dow Chemical Company. A numerical "fire and explosion index" (F & EI) is calculated, based on the nature of the process and the properties of the process materials. The larger the value of the F & EI, the more hazardous the process.
Judgment, based on experience with very similar processes, is needed to decide the magnitude of the various factors used in the calculation of the index, and the loss control credit factors.

What If Analysis is a structured brainstorming method of determining what things can go wrong and judging the likelihood and consequences of those situations occurring. The answers to these questions form the basis for making judgments regarding the acceptability of those risks and determining a recommended course of action for those risks judged to be unacceptable.

2.2.1.2 The semi-quantitative methods

The semi-quantitative approaches are: HazOp (Hazard and Operability study), FMEA (Failure Mode and Effect Analysis) and FMECA (Failure Mode, Effect and Criticality Analysis).

A hazard and operability study is a systematic procedure for critical examination of the operability of a process. When applied to a process design or an operating plant, it indicates potential hazards that may arise from deviations from the intended design conditions and it can help in the individuation of the "top events", that are the possible incident or accident events. The technique was developed by the Petrochemicals Division of Imperial Chemical Industries, and is now in general use in the chemical and process industries.

A formal operability study of the design, vessel by vessel and line by line, using "guide words" to help generate thought about the way deviations from the intended operation can cause hazardous situations. The seven guide words recommended are given in table 2.1. In addition to these words, the following words are also used in a special way, and have the precise meanings given below:

- *Intention:* the intention defines how the particular part of the process was intended to operate;
- *Deviations:* these are departures from the designer's intention that are detected by the systematic application of the guide words;
- *Causes:* reasons why, and how, the deviation could occur;
- *Consequences:* the results that follow from the occurrence of a meaningful deviation.
- *Hazards:* consequences that can cause damage (loss) or injury.

Table 2.1. *A list of guide words with their meaning and comments.*

GUIDE WORD	MEANING	COMMENTS
NO	Complete negation, e.g. of INTENTION	NO forward flow when there should be
MORE	Quantitative increase	MORE of any relevant physical property than there should be (e.g. higher flow, temperature, pressure, viscosity, etc. also actions: heat and reaction)
LESS	Quantitative decrease	LESS of … (as above)
AS WELL AS	Quantitative increase	All design and operating INTENTIONS are achieved together with some addition (e.g. Impurities, extra phase)
PART OF	Quantitative decrease	Only some of INTENTIONS are achieved, some are not
REVERSE	Opposite of INTENTION	Reverse flow or chemical reaction (e.g. inject acid instead of alkali in pH control)
OTHER THAN	Complete substitution or miscellaneous	No part of original INTENTION achieved, something quite different occurs. Also start-up, shutdown, alternative mode of operation, catalyst change, corrosion, etc.

Failure-mode effect analysis (FMEA) is a method originally developed in manufacturing, which is used to determine the relative importance of different component failures within an overall system or product. It assigns numerical rankings to different failure modes based on the (qualitative) perceptions of the participants. Different groups or individuals will not necessarily reach the same conclusions, so the method is best used in the early stages of design as a means of brainstorming for safety issues. More rigorous methods such as HazOp should be applied when more design details are available.

2.2.2. Quantitative hazard analysis

Methods such as FMEA, HazOp and use of safety indices will identify potential hazards, but give only qualitative guidance on the likelihood of an incident occurrence and the loss suffered. In a quantitative hazard analysis, the engineer attempts to determine the probability of an event occurring. The most used quantitative approaches are the fault tree and the event tree.

2.2.2.1. Fault tree

Incidents usually occur through the coincident failure of two or more items: failure of equipment, control systems and instruments, and mis-operation.

The fault tree analysis (FTA) is a deductive ("Top-Down") procedure that examines the sequence of events leading to the top event, a hazardous incident. It starts from the top event (TE), identified for instance during the HazOp analysis, and, asking for what failure can cause it, arrives to the initiator events (the breakdowns, the faults).

In figure 2.2 there is an illustrative example of a fault tree.

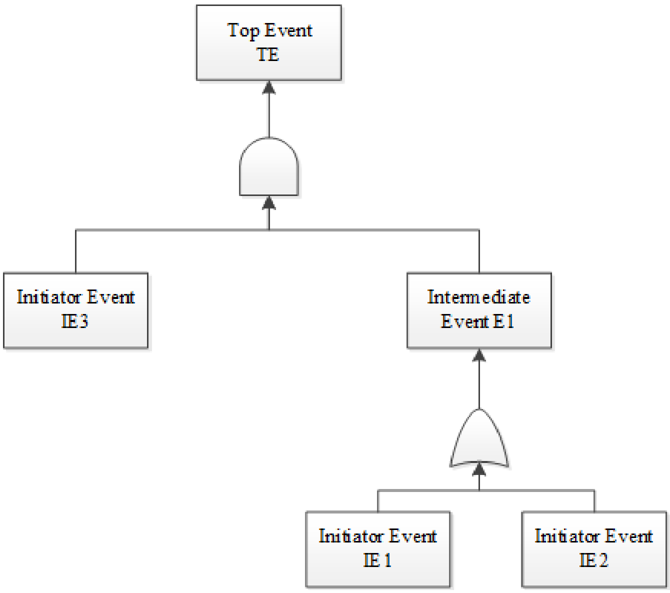

Figure 2.2. *Example of a fault tree. Letter A stands for AND operator, letter B stands for OR operator.*

This method is useful because it permits not only to have a representation of the paths necessary to obtain the TE but also to estimate its occurrence probability. This is possible to realize when the failure frequencies or probabilities of each initiator event are known. The frequency determines the number of failures in a defined period of time while the probability is a dimensionless number. These values can be combined adopting the Boolean algebra. In the fault tree, two are the most used logical gates: AND and OR. The AND logical operator is used where all the inputs are necessary before the system fails, and the OR logical operator where failure of any input, by itself, would cause failure of the system. If the events (initiator or intermediate) are connected with an AND logical operator, the probability (frequency) of the output event is calculated as the product of the probability (frequency) of all input events; while, if an OR logical gate is used, the output event probability (frequency) is calculated as the sum of all input events probabilities (frequencies).
The equation to calculate the frequency of the top event (TE) of the Figure 2.2 is:

$$TE = IE3 \cdot E1 = IE3 \cdot (IE1 + IE2)$$

The fault tree analysis is deterministic since a mean value of failure frequency is taken into account for each initiator event.

2.2.2.2. Event tree

An event tree analysis (ETA) is an inductive procedure ("Bottom-Up") that shows all possible outcomes resulting from an accidental (initiating) event and additional events and factors. By studying all relevant accidental events (that have been identified by a preliminary hazard analysis, a HazOp, or some other technique), the ETA can be used to identify all potential

accident scenarios and sequences in a complex system. Unlike the fault tree analysis, in which the top event has to be stated, in the event tree analysis the starting point is an initial event, which is the release of some dangerous substance (toxic, flammable or explosive) in most cases. Then it's possible to identify the direct consequences (fires, explosions, toxic emissions, etc.) or the indirect ones (for example the domino effect). The event tree is composed of nodes and each node represents a different question to which the only possible answers are yes or no; it's possible to build a very branched tree defining and responding to all questions that can influence the development of the initial event into the final event (the accidental scenario).
Design and procedural weaknesses can be identified, and probabilities of the various outcomes from an accidental event can be determined.
In Figure 2.3 there is an example of an event tree.

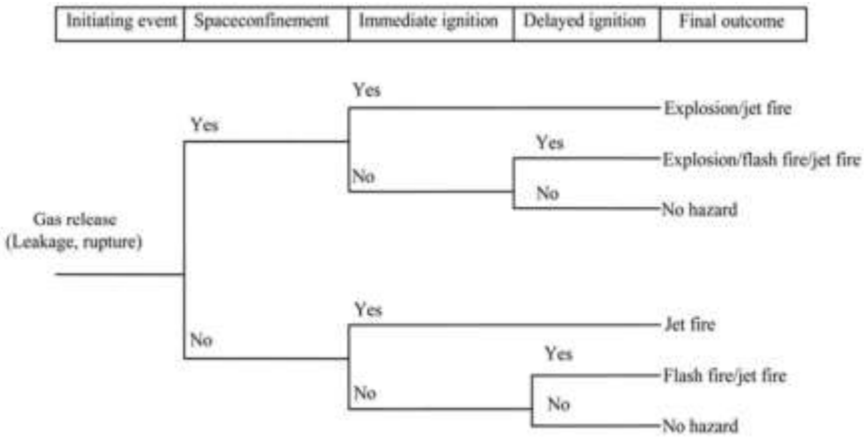

Figure 2.3. *Example of an event tree.*

2.2.2.3. Bow-Tie diagram

The Bow-Tie diagram represents the fault tree and the event tree together. It is suitable to visualize the relationship between undesirable event, its causes, accidental scenarios and their consequences.
In Figure 2.4 there is a scheme of a bow-tie diagram.

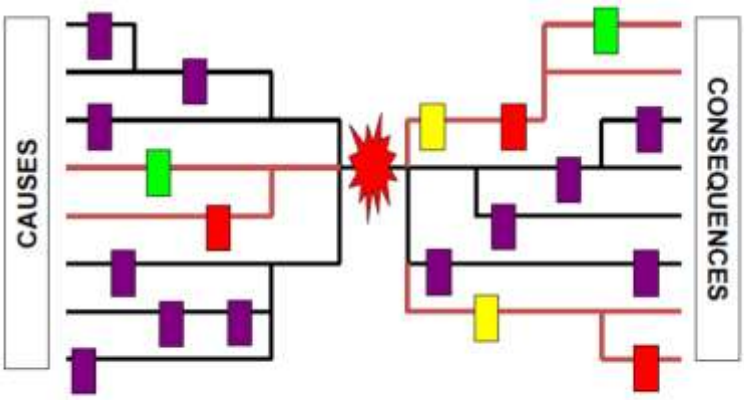

Figure 2.4. *Scheme of a bow tie diagram*

As it can be seen in Figure 2.4, in the middle of the scheme there is the critical event (CE), while the left part is the fault tree, that identifies the possible causes of the CE, and the right part is the event tree, that, indeed, identifies the possible consequences of the CE. The bow-tie technique in its visual form makes the analysis easy to understand, and can show what safeguards protect against particular initiating causes and loss event consequences.

Chapter 3

Modification on the classical risk assessment

The aim of this chapter is to highlight the limitations of the conventional risk assessment and to present how it can be modified, in such a way that also the so called atypical events can be considered.

3.1 Limitations of the Hazard Identification

In the previous chapter the approaches to carry out the Hazard Identification were itemised and explained. But none of them seems to cover the issue of accident scenarios falling out of normal expectations of unwanted events and their dynamical integration into Hazard Identification (HazId) process. Furthermore, Hazard Identification should face some theoretical and practical limitations that affect the quality of the results. The Centre for Chemical and Process Safety identifies five main limitations in the application of Hazard Identification techniques:

i) *Completeness*: some accident situations, causes, and effects may have been unintentionally neglected;

ii) *Reproducibility:* assumptions from the analyst may affect results;

iii) *Inscrutability:* results may be difficult to understand and synthesize for use;

iv) *Relevance of experience:* lack of specific experience may lead to neglect the significance some aspects;

v) *Subjectivity*: since analysts may have to use their judgment when extrapolating from their experience).

Some of these limitations significantly hinder the identification of “atypical” accidents scenarios.

3.1.1 “Atypical” accident scenarios

Since 1976, when the major accident of Seveso (Italy) occurred, it was clear how complete and effective activities of appraisal and assessment of potential hazards in the process industry are of primary importance for the prevention of such accident scenarios. In fact, what remains unidentified cannot be prevented or mitigated and a latent risk is more dangerous than a recognized one due to the relative lack of emergency preparedness.

This type of scenarios can be classified as “atypical” because they cannot be captured by standard risk analysis processes and common HazId techniques due to their deviation from normal expectations of unwanted events or worst case reference scenarios.

Another latent risk can be represented by the accident scenarios related to new and emerging technologies, which are not still properly identified, and that may remain unidentified until they take place for the first time. Examples of new and emerging technologies can be found within the fields of Liquefied Natural Gas (LNG) regasification and Carbon Capture and Storage (CCS), where new and alternative technologies are being defined and the scale and extent of both the substances (LNG and CO_2) handling is set to increase dramatically. Thus, a lack of substantial operational experience may lead to difficulties in identifying accurately the hazards associated with the process. Hence, these new and emerging hazards may comply with the definition of “atypical” scenarios previously discussed.

Furthermore, industrial risk assessment should take account of consequences and probability of occurrence of accidental scenarios triggered by natural events.

Atypical events may be classified in two separate groups:

- *“Unknown Unknowns”*: these are the type of events that have never occur or for which there is no available information;
- *“Unknown Knowns”*: these are events that the risk analyst is not aware could know considering near misses or past accidents.

Risk awareness is a fundamental factor to tackle the issue of atypical accident scenarios and, together with an effective knowledge management, would make possible the achievement of a complete and effective process of risk management. Moreover, when dealing with atypical scenarios, it should not be forgotten that an accident affecting a complex system is a multiple and unexpected interaction of failures and there is not one single cause.

The implementation of a strong safety culture within the plant is of paramount importance for the prevention of unforeseen events, especially for “Unknown Unknowns”. One way to deal with this problem is to improve early detection of deviations in the causal chain by means of specific monitoring systems. In fact, the development of appropriate proactive indicators would help to increase organizational awareness (mindfulness) of safety and reduce complacency in organizations where major accidents are possible but rare.

To face “Unknown Knowns” a comprehensive process of identification based on early warnings, capturing evidence of new hazards to consider as soon as they come to light, is essential.

Conventional risk assessment has the disadvantage of being static and fails to capture emergence of new hazards. For this reason, a specific method named Dynamic Procedure for Atypical Scenarios Identification (DyPASI) was developed to obtain comprehensive hazard identification including Atypical Scenarios.

3.2 Dynamic Procedure for Atypical Scenarios Identification (DyPASI)

DyPASI is an HazId method aiming at the systematization of information from early signals of risk related to past accident events, near-misses and risk studies. It supports the identification and the assessment of atypical potential accident scenarios related to the substances, the equipment and the industrial site considered.

The application of DyPASI entails a systematic screening process that, based on early warnings and risk notions, should be able to identify possible Atypical Scenarios or Unknown Knowns available at the time of the analysis. The well-established approach of the bow-tie analysis, which aims at the identification of all the potential major-accident scenarios occurring in a process industry, was taken as a basis to develop the methodology. A general flow-chart of the methodology is provided in Figure 3.1, that also evidences its integration in the risk management framework.

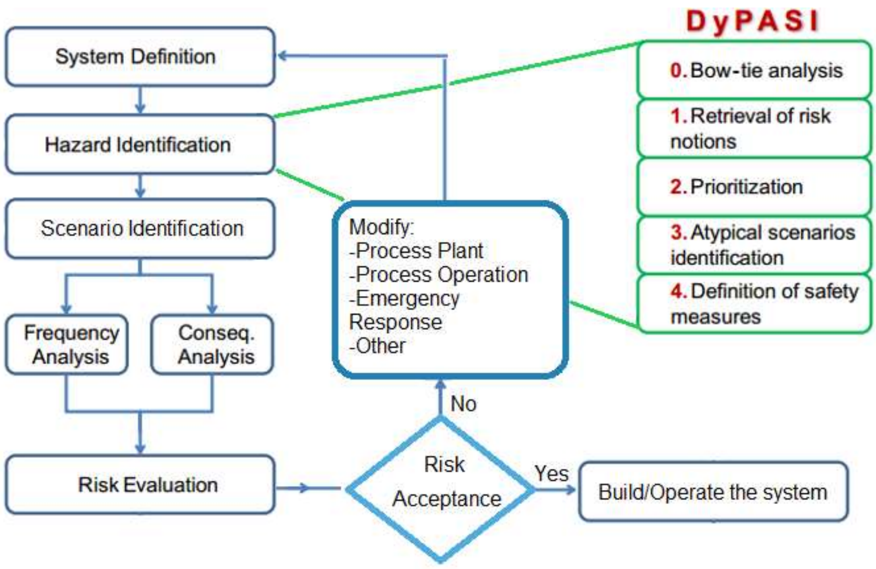

Figure 3.1. *DyPASI steps and their inclusion in the process of risk assessment.*

DyPASI may be used either as a stand-alone HazId technique or may be coupled with existing conventional techniques. In the latter case, it may effectively integrate the existing hazard identification methods to obtain more exhaustive results. In particular, it provides a structured and yet dynamic approach in the retrieval of information from early warnings and atypical scenarios, which is not present in the conventional application of other HazId techniques.

The format of the results from DyPASI allows for a particularly easy integration with the HazId techniques based on fault tree and event tree analysis, effectively extending the applicability of DyPASI from the preliminary analysis to the assessment of detailed plant systems.

3.2.1 Bow-tie analysis

DyPASI is a development of the bow-tie technique, which, by itself, is a qualitative hazard evaluation technique ideally suited for the initial analysis of an existing process or application during the intermediate stages of process design. Thus, as a preliminary activity (step 0) DyPASI requires the application of the conventional bow-tie technique to identify the relevant critical events. The development of bow-ties can be performed following conventional guidelines as those outlined by the Centre for Chemical Process Safety or the MIMAH tool.

3.2.2 Retrieval of risk notions

In the first step of DyPASI application, a search for relevant information concerning undetected potential hazards and accident scenarios that may not have been considered in conventional bow-tie development is carried out. It can be summarized in 3 steps:

- Definition of the information need and search systems to search on
- Formulation of a query to send to the search system
- Assessment of the relevance of results

Search boundaries must be outlined and quoted in the formulation of the query, in the combination and number the analyst considers more appropriate. Examples of search boundaries used in queries are: the site, the process, the equipment, the substance, and the substance state.

3.2.3 Prioritization

Once the necessary information is gathered, a determination is made as to whether the data are significant enough to trigger further action and proceed with the process of risk assessment. As a support of this process of prioritization (step 2 of DyPASI application), a register collecting the risk notions obtained from the retrieval process and showing their relative relevance and impact can be obtained. Possible consequences can be determined based on the risk notions and ranked by means of the following scale of severity levels:

- *Near miss*: an event that does not result in an actual loss but that has the potential to do so.
- *Mishap*: an event that could cause minor health effects and/or minor impact to property and the environment.
- *Incident*: an event that could cause major health effect or injury, localized damage to assets and environment, considerable loss of production and impact on reputation.
- *Accident*: an event that may cause one or more fatalities or permanent major disabilities, and/or heavy financial loss.

- *Disaster*: an event that could cause multiple fatalities and extensive damage to property, system and production. It may cause a shutdown of the plant for a significant time period and sometimes forever.

Step 2 describes a qualitative prioritization of severity. It will be a task of the user of DyPASI to extrapolate early warnings of a potential atypical accident scenario. The classification of gathered data performed on the basis of relevance and impact will help the user to identify the most pertinent and serious signals.

3.2.4 Identification of atypical scenarios

In this step, the potential scenarios are isolated from the early warnings gathered and a cause-consequence chain consistent with the bow-tie diagram is developed. This allows for the integration of the pattern of the atypical scenario the bow-tie of hazards previously identified at step 0.

There are many well-known methodologies for past accident analysis that can be applied to obtain a reduction to a cause-consequence chain consistent with the bow-tie diagram characteristics. This procedure suggested within DyPASI takes indication from the *Why Tree* technique. At first, the Basic Event (BE), the Critical Event (CE) and the Outcome Event (OE), which are the main elements of a bow-tie diagram, must be identified within the potential atypical scenario. Then, the other elements are defined asking the question "why?", or, more specifically "what is directly necessary and sufficient to cause this event?", starting from OE and going backward through CE until BE. The number of the "Intermediate Events" and "Events" can vary for other techniques of bow-tie analysis.

Once a specific pattern to describe the atypical scenario is defined, one or more suitable bow-tie diagrams obtained in step 0 may be identified for the process of integration. The specific search boundaries used in the previous steps and the defined CE should be used for the identification of appropriate bow-tie diagrams. If no suitable diagram is identified, the atypical scenario pattern must be considered a new bow-tie diagram itself, which should be added to the set of HazId results.

The process of integration of an atypical scenario in a bow-tie diagram may be obtained by a specific methodology based on set theory. The approach is able to ensure complete and concise results, without the need to re-develop a HazId study from the beginning.

The integration of the atypical scenario pattern should be performed considering one half of the diagram at a time and should move level-by-level from the CE to the BE (if the fault tree section is considered) or OE (of the event tree is considered). Regarding Figure 3.2, the following guidelines must be applied for each event level:

1) If $E_{Aty,n}$ (it's the set of atypical events $e_{Aty,n}$in the event position n) is a subsystem of $E_{ini,n}$ (it's the set of initial events $e_{ini,n}$ in position n; that is $E_{ini,n} = E_n$) and ∃ a

function f: $E_n \rightarrow E_{n-1}$ surjective (it means that per each initial event $e_{ini,n-1}$ exists $e_{ini,n}$) ⇒ consider next level (n+1)

2) If $E_{Aty,n} - E_{ini,n} \neq \emptyset$ ⇒ integrate it and consider $E_n = E_{Aty,n} \cup E_{ini,n}$
3) If f: $E_n \rightarrow E_{n-1}$ is not surjective ⇒ duplicate $e_{Aty,n}$| f becomes surjective

For n=1…, N event levels.

E_n is the set of all events and the initial events are events identified with the conventional hazard identification.

The scheme of the right-hand part of a bow-tie diagram using the three guidelines is shown in Figure 3.2.

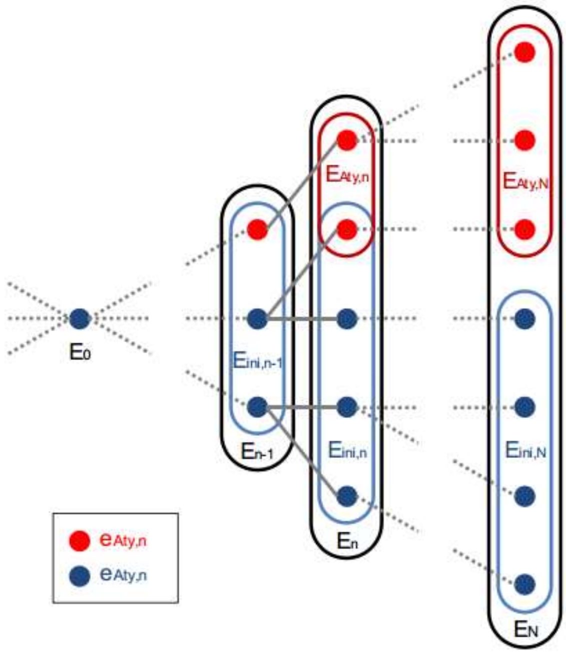

Figure 3.2. *Scheme of the right-hand part of the bow-tie diagram using the three guidelines; the Critical Event is in position n=0 and the outcome events in position n=N.*

3.2.5 Identification of safety measures

The definition of safety measures applied to the elements of bow-tie diagrams is the last step of the DyPASI procedure. In this step, past experience concerning the effectiveness and performance of safety barriers may be encompassed in the analysis.

The integrated bow-tie diagrams including the atypical scenarios should be completed considering safety barriers, classified by their effectiveness. The generic safety functions can be divided into these four actions to be achieved:

- Measures to avoid: safety function acting upstream of the bow-tie diagram event aiming to suppress the inherent conditions that cause it.

- Measures to prevent: safety function acting upstream of the bow-tie diagram event aiming to reduce its occurrence.
- Measures to control: safety function acting upstream of the fault tree event in response to a drift which may lead to the event and safety function acting downstream of the event-tree event aiming to stop it.
- Measures to limit: safety function acting downstream of the bow-tie diagram event aiming to mitigate it.

The safety barriers can be physical and engineered systems or human actions based on specific procedures, or administrative controls which can directly implement the safety functions described.

DyPASI introduces a further distinction between safety barriers represented in the bow-tie diagram: safety barriers properly acting should be marked in green (green colour is also applied to effective safety barriers in the case of near-misses); safety barriers that showed deficiencies in at least one past accident are marked in orange; new potential, and hopefully more effective, safety barriers identified are represented using the red colour.

This activity can also provide important elements for the risk mitigation process in the decision-making phase of risk management.

3.3 Quantitative Risk Assessment (QRA)

As soon as the integrated bow-ties are available, the follow-up consists in carrying out the conventional risk management procedure.

Quantitative Risk Assessment (QRA), once potentially hazardous events are identified, is a formal and systematic approach of estimating their likelihood and consequences, and expressing the results as risk to people, the environment or the infrastructures.

The main result of a QRA is the estimation of failure frequency values, which usually is derived by coupling results provided by the fault tree analysis, which mainly takes into account anomalies of mechanical components, control and protective device as main failure cause, and the event tree analysis, performed to define potential damage consequences induced by each identified top event.

The QRA approach is deterministic since a mean value of failure frequency is considered for each initiator event. If seismic risk is concerned, the deterministic approach is based on the maximum “credible” intensity of earthquake as the triggering event and a conservative estimate (“worst case” assumption) for the subsequent accidental scenario is made depending on the interaction of the earthquake shaking with equipment, which can result in a loss of material or energy. In the above form, the deterministic approach leads often to a significant overestimation of the risk, so that such a risk grade becomes both economically and politically not sustainable, e.g. in the case of civil protection action. Moreover, the uncertainties related to the initial conditions of the seismic scenario, to the failure of equipment, and to the uncertainties in the analysis of consequences of the possible destructive phenomena following the loss of hazardous substances are often too large.

3.3.1 Probabilistic fault tree framework

Thus, it's evident that the classical quantitative risk analysis doesn't provide a complete investigation since it doesn't consider uncertainties related in the estimation of temporal occurrence of each singular initiator event and, in addition, natural hazards are not frequently considered in QRAs due to challenges related to the evaluation of their consequences in the chemical process industry.
These circumstances lead analysts to use a probabilistic approach, where uncertainties are explicitly considered and described by probability distributions.

3.3.1.1 Primary failure probability estimates

The commonly used techniques to estimate primary failure probabilities are mainly based on generic data available in literature, specific studies and reliability. Data are deterministic, so failure frequencies are average values derived from dataset of past accidents, without taking into account any variability in frequency estimation.
In the probabilistic fault tree framework, frequency mean value data and related standard deviations are indeed used to build probability density functions of the frequency values associated to each initiator event. A lognormal function is assumed for each initiator event frequency. A set of *n* simulations is performed for estimating component release probabilities. For each random simulation, a i^{-th} frequency value λ_i is sampled from each frequency probability density function. Finally, the probability values $P_i(\lambda_i)$ are subdivided according to LNE Department (2009) into three possible release states (*RS*) as follows:

- $P_{i,RS1}(\lambda_i)$ corresponding to *RS1*, (i.e. small release), estimated as 84% of $P_i(\lambda_i)$;
- $P_{i,RS2}(\lambda_i)$ corresponding to *RS2*, (i.e. moderate release), estimated as 8% of $P_i(\lambda_i)$;
- $P_{i,RS3}(\lambda_i)$ corresponding to *RS3*, (i.e. high release), estimated as 8% of $P_i(\lambda_i)$.

3.3.1.2 Seismic probability estimates

Chemical plants can be subject to an increase of failure rate if located in areas prone to seismic hazard. In such cases, release can be a direct consequence of earthquake-induced structural failure of tanks, pipes and other elements drift- or acceleration- sensitive.
Hence, seismic hazard must be adequately taken into account in probabilistic terms since earthquakes can occur at several sites and can be characterized by different magnitudes following specific recurrence laws.
If a structural component is located in a site, it is possible to define its seismic hazard curve

according to the results provided in the National Building Codes with regard to Probabilistic Seismic Hazard Analysis. The goal of *PSHA* is to estimate the probability of exceeding various ground-motion levels given all possible earthquakes that could affect the site of interest in a preset time window *T*.

For each ground motion level, by fixing a preset time window and selecting a specific intensity measure, it is possible to perform the seismic hazard disaggregation analysis. Seismic hazard disaggregation allows engineers to identify the values of some characteristics earthquakes that provide the largest contributions to the hazard at a specific site of interest. These events can be viewed in probabilistic terms as the *k* earthquakes dominating the seismic hazard of a site.

Once identified such *k* scenarios in terms of event magnitude *M* and epicenter distance *R* from the site of interest, it is possible to define for each of them a lognormal probability distribution of the selected intensity measure through a Ground Motion Prediction Equation (*GMPE*). On such basis, also in this case, a set of *n* simulations are performed for estimating component release probabilities. For each i^{-th} simulation, *k* intensity measure values $IM_{i,x}$ are randomly sampled by respective *GMPE* probability density functions.

Once desegregated seismic hazard, the following step is the assessment of probabilities of detecting a certain damage state: in this regard, seismic vulnerability of chemical plant component can be described, as said in Chapter 1, through fragility functions, representative of exceedance probability values for a set of possible damage states as a function of a specific intensity measure value to which an element is subject during an earthquake.

In the framework of the *QRA*, the estimation of loss of hazardous materials is the most challenging issue but it is necessary for properly assess consequences of potential failures. Hence, structural damage states must be converted in terms of release states *RS*, which are the same of that previously described. In such way fragility curves in terms of exceedance probability of a set of possible release states (*RS1*, *RS2*, *RS3*) are taken into account, adopting fragility coefficients reported in Tables 1.2 and 1.3.

So for each intensity measure value $IM_{i,x}$, *RS1*, *RS2* and *RS3* release state probabilities $P_{i,RSj}$ ($IM_{i,x}$) are computed: for each i^{th} simulation, all these values are then condensed taking into account disaggregation percent contributions $\%_x$ of each k^{th} considered event, as follows:

$$P_{i\,,RS_j} = \sum_{x=1}^{k} (\%_x) \cdot P_{i\,,RS_j}\,(IM_{i,x}) \cdot \frac{1}{T_{R,x}}$$

where $T_{R,x}$ is the return time of each considered event.

3.3.1.3 Final probability aggregation

The last step of the probabilistic fault tree analysis method is the aggregation of probability values derived from the primary and the seismic failure estimates. Release probability values derived in the i^{th} simulation from the electro-mechanical initiator events branch and earthquake occurrence branch are thus processed according to the fault tree diagram (taking into account logical operators AND, OR) to derive a final set of aggregate release probability values for *RS1*, *RS2* and *RS3*. The analysis is repeated performing *n* simulations and thus leading to define release probability value distributions for each release state analyzed.

Chapter 4

Case study – DyPASI analysis

It's considered the Green Refinery of Porto Marghera, in particular it's taken into account the storage section S-111.
In order to apply the modified risk analysis, it's important to decide where to place the plant and then study the vulnerability of the plant site. Afterwards it's possible to apply the DyPASI analysis with the aim of including the NaTechs in the risk assessment. Once the bow-tie is updated, the last step, that is submitted in Chapter 5, is the quantitative risk assessment done in probabilistic terms.

4.1 The plant

In this thesis, it's considered the Refinery of Porto Marghera (VE). In 2013, the Refinery of Porto Marghera decided to integrate the conventional refinery scheme with the plan of a "Green Refinery", that allow the production of high-quality innovative biofuels (such as Green Diesel, Green LPG and Green Naphtha) from biomasses. In Figure 4.1 it's shown the block flow diagram of the process that produces the green diesel.

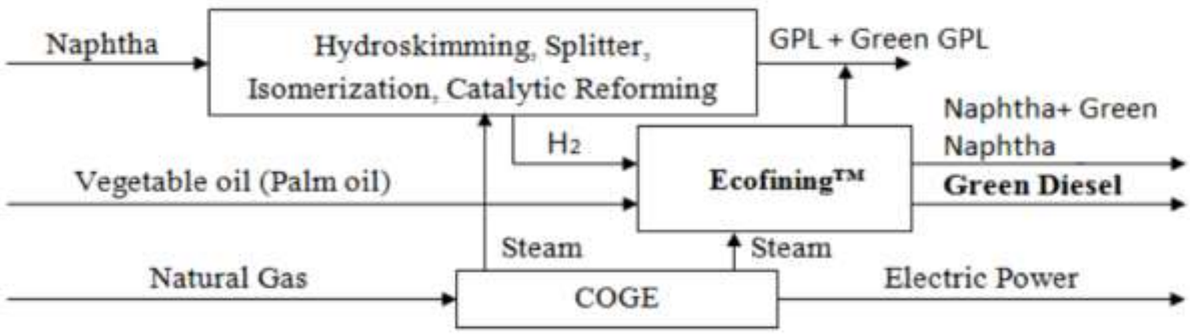

Figure 4.1. *Block flow diagram of the plant.*

The Ecofining™ technology is based on two steps:

- the hydro-deoxygenation, where the oxygen is removed and a linear paraffinic hydrocarbon, with poor cold properties, is produced;
- the isomerization, that is necessary to improve the cold properties of the fuel and so a paraffinic hydrocarbon with branched chains is obtained.

The case study is focused in the storage S-111 used to stock the produced green diesel after the isomerisation step and it’s shown in Figure 4.2.

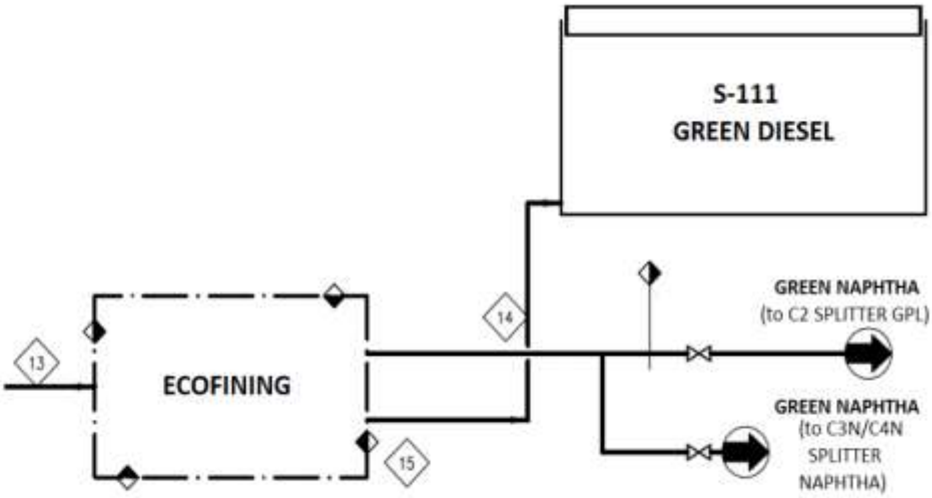

Figure 4.2. *Green diesel S-111 storage graphic representation.*

4.2 Plant location

The purpose of this thesis is to study and to add the seismic risk within the risk analysis, thus the choice of the location of the plant is a key point.

In seismic terms, Italy has three great areas. It is visible in Figure 4.3 that the high-risk areas are Apennines, Sicily and Friuli.

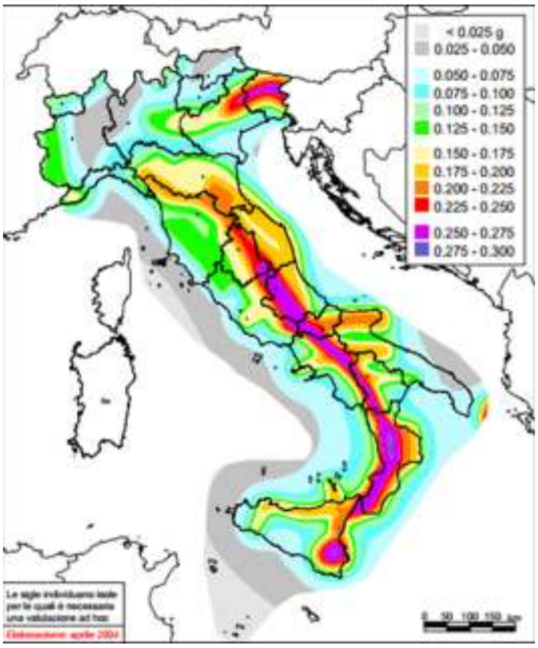

Figure 4.3. *Seismic map of Italy. The legend expresses all the PGAs in terms of g. Two great seismic areas are along Apennines and in Friuli, due to orogeny.*

This hazard is due to the orogeny mechanism: in these areas, there are relatively young mountains, created by the clash between the Euro Asiatic plate and the African one. For this reason, in order to study the effects of an earthquake on an industrial production, it is important to choose wisely the location.

In this work, two locations for the plant are chosen: the first option is the "original" one in Porto Marghera (VE), and the second option is in Priolo Gargallo (SR).

The next step is the application of DyPASI technique, but before analysing the possible NaTech scenarios, it's important to study the vulnerability of the plant site.

The vulnerability of an area is the propensity to be subjected to damages by a specific phenomenon; it represents the lack of resilience or, in other words, the capability to absorb impacts and contrast adverse events.

4.2.1 Porto Marghera vulnerability

The green refinery is located in the industrial site of Porto Marghera and the surrounding urban area are: Mestre at 3 km, Marghera at 2.6 km and Venice at 4 km.

So, the green refinery is placed closed to urbanized areas and to Venice that is Unesco heritage. Furthermore, there is another element that has to be taken into account: the vulnerability related to adverse natural events. These aspects are significant to understand the territorial vulnerability in which the green refinery have to work and so the absolute importance of an adequate and complete risk assessment and management.

The first natural phenomenon considered to evaluate the vulnerability of the site is the earthquake. According to the last seismic classification of the Civil Protection (2015), Venice is classified with the fourth level and so with the lowest probability of occurrence of earthquake, as can be shown in the Figure 4.4.

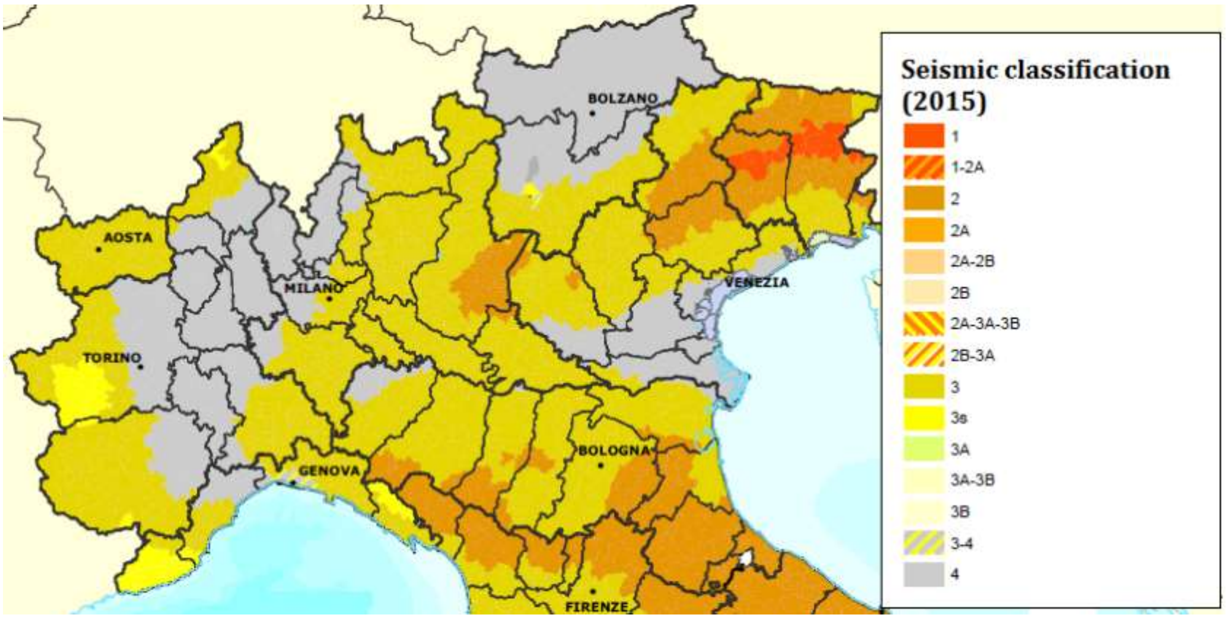

Figure 4.4. *Seismic classification (2015) of the North-Italy.*

Nevertheless, it's important to observe that several earthquakes, as that of the 20th May 2012 in Emilia, cause enormous consequences even though classified with low seismic level (in the example of Emilia the region was classified as level three); moreover, heavy consequences can be caused by a seismic activity that has the epicentre in another region but with a magnitude that is too high.

Other natural events are rainfall and tornado that are considered in the report of Veneto regional council (2012). The report is focused especially on these events due to the several disasters caused by the flood rain in 2010. In the last years, it is highly discussed about the "flash-flood" or in other words, high intensity rainfall with following storms that cannot be prevented with current meteorological and hydrological models and that could be a consequence of the global warming. In fact, if on one hand there is a decreasing of the annual and winter rainfall, on the other hand it's possible to observe the above-mentioned "flash-flood" events or rather intensive rainfall in the hot semester of the year (May-October). Adopting the CI (a normalized concentration index), that estimates the concentration of the daily rainfall, it's possible to observe in Figure 4.5 how this index is increased in the last 20 years and how its territorial distribution is changed; it's clear to understand that in Porto Marghera site there is an increasing of the intensity of rainfall.

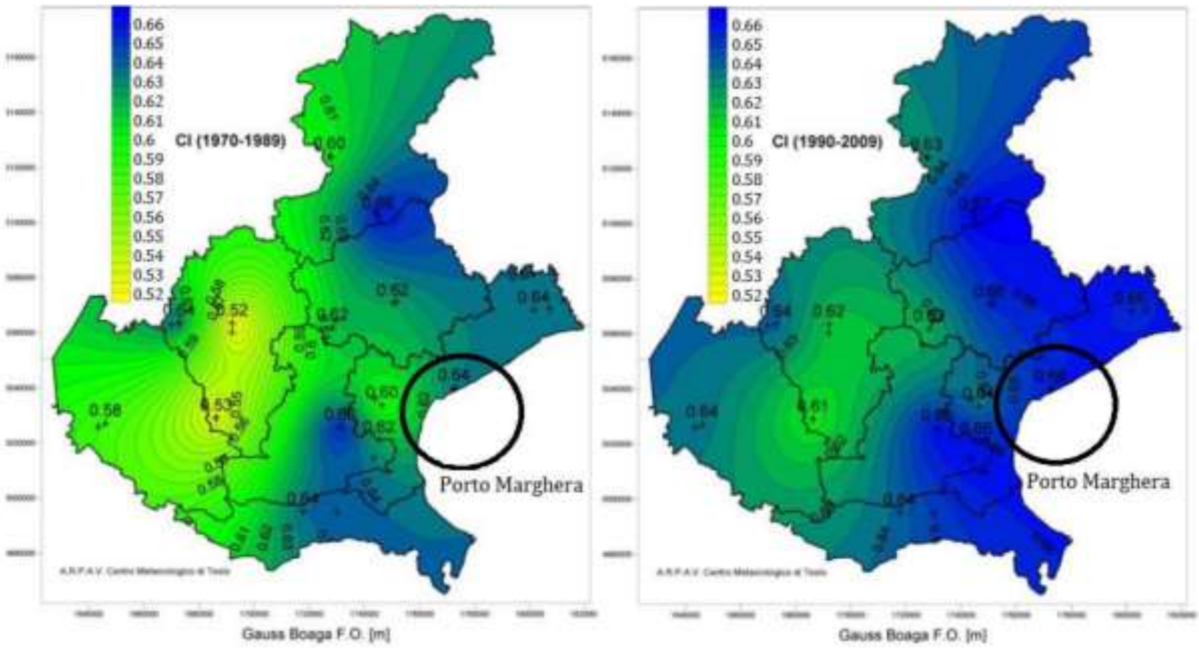

Figure 4.5. *Change in the CI value from 1970-1989 to 1990-2009 period.*

About Marghera in particular, in Figure 4.6 it is possible to show the special rainfall of the 26th September 2007 in Mestre and Marghera, when the total precipitation in 12 hours was ~260 mm.

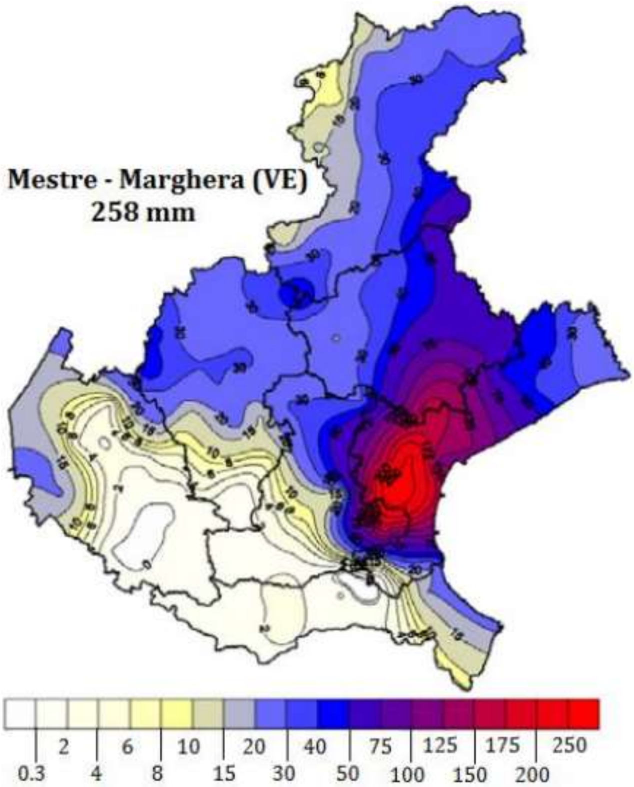

Figure 4.6. *Special rainfall in Mestre and Marghera in the 26th September 2007.*

If the classification of the daily precipitation adopted by Veneto is taken into account, it's possible to conclude that the special event of the 26th September 2007 falls into the extreme class (it's the class 5 and considers a precipitation > 70 mm/day); these and other events demonstrate that extreme rainfalls are becoming quite likely. This information is important to evaluate the reliability or not of NaTech caused by heavy rain and that can have negative effects for the green refinery. Even tornado and downburst (storm wind) are increasing (in Veneto and especially near Porto Marghera area) as can be demonstrated by some episodes as the downburst in Mestre in 15th June 2007 that caused 30 injured. It's important to underline that these and the rainfall considerations would require more data estimated in a long period of time; so, it's not scientifically exact to draw conclusions on these few data but, to achieve the aims of the topic, they can be sufficient.

It's also important to underline that Veneto is one of the region more affected by lightning as it's shown in Figure 4.7, where is estimated a frequency of occurrence greater than 4/ ($km^2 \cdot$ year) as defined by the CEI 81.8.

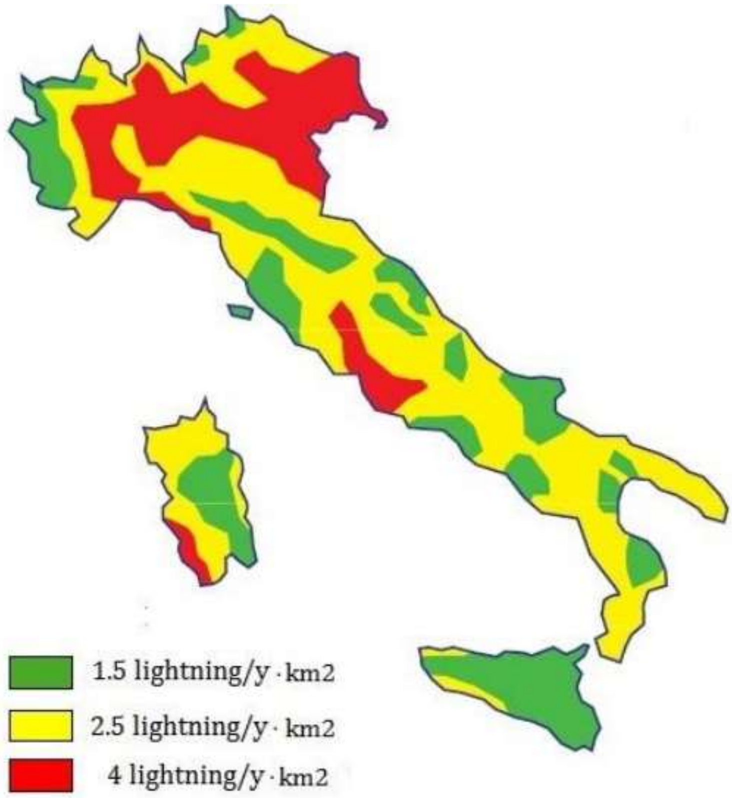

Figure 4.7. *Italian area classification of lightning activity.*

This is another natural event that causes several NaTech all around the world. It's possible to observe in the Figure 4.8 and 4.9, reported by Necci Amos (2015), the number of accidents for plant and equipment type.

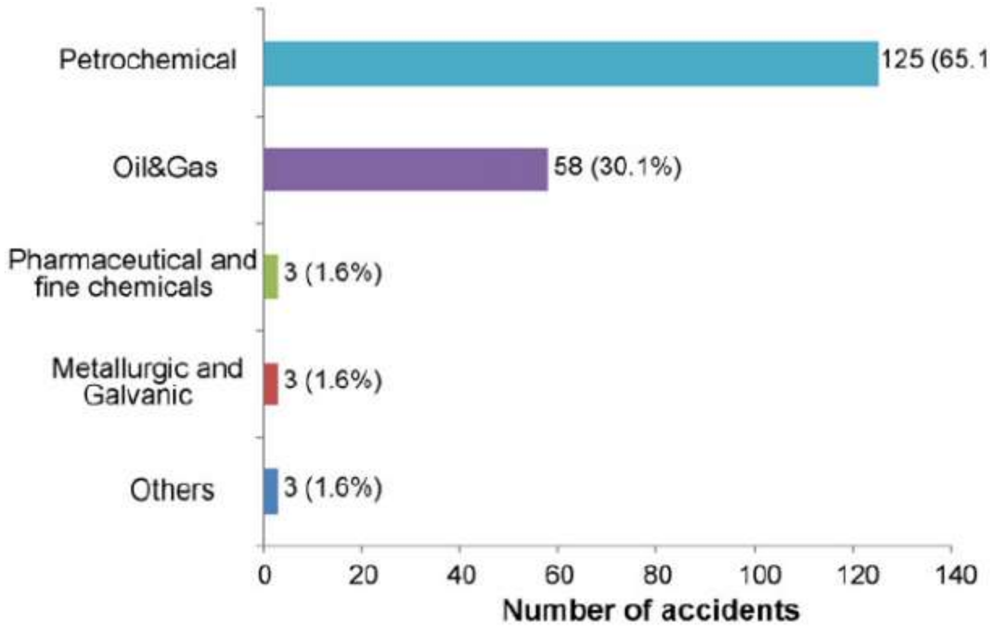

Figure 4.8. *Industrial activities involved in lightning-triggered accidents.*

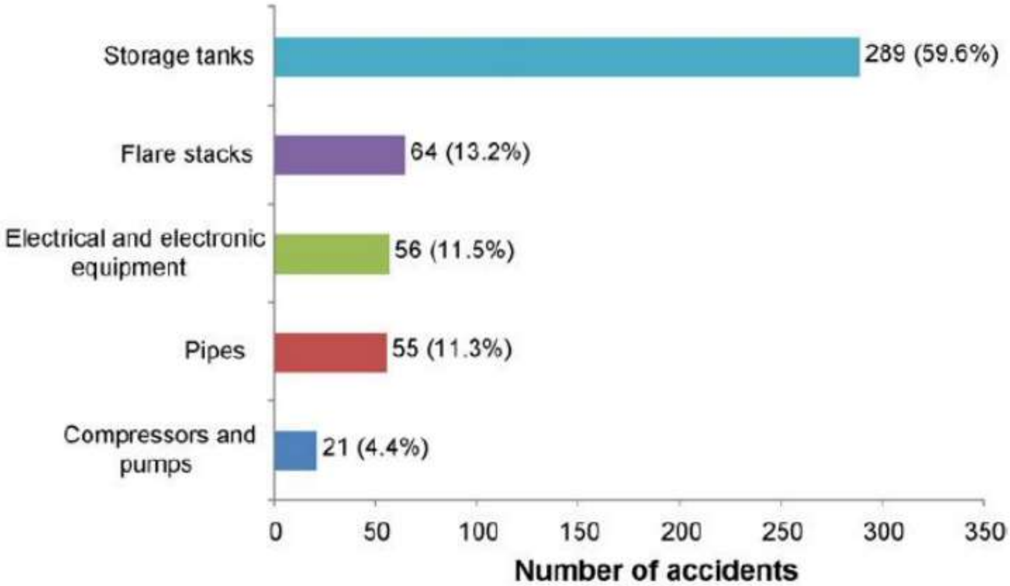

Figure 4.9. *Equipment categories involved in Natech accidents due to lightning*.

It’s clear to understand that petrochemical and oil & gas plants are the most vulnerable while the most damaged equipment type is the storage tank.

The final natural phenomenon that is analysed is the high tide with possible following floods. This type of event is neglected from this analysis because of the position of the green refinery; in fact, the site isn’t affected by flood due to the high tide as is possible to demonstrate with the absence of consequences in the case of the extraordinary event of the November 1966, when a level of +194 cm was reached.

4.2.2 Priolo Gargallo vulnerability

It’s then considered the location of the plant in Priolo (SR), a town in Sicily. This choice is not casual: the natural conformation of the place, with a large gulf perfect for a harbour, was chosen in 1949 for one of the biggest industrial district of Italy. What was not taken into account is the seismic danger of the area. This risk has two components: the first one is due to the collision between the Euro Asiatic and the African plaques (the so called “faglia dello Stretto” and “Ibleo Maltese”), the second is the presence of Mount Etna, the major active volcano in Italy. This combination of factor originates one of the highest seismic risk area of Italy. In Figure 4.10 it’s shown the seismic classification of the Civil Protection (2015) of Sicily.

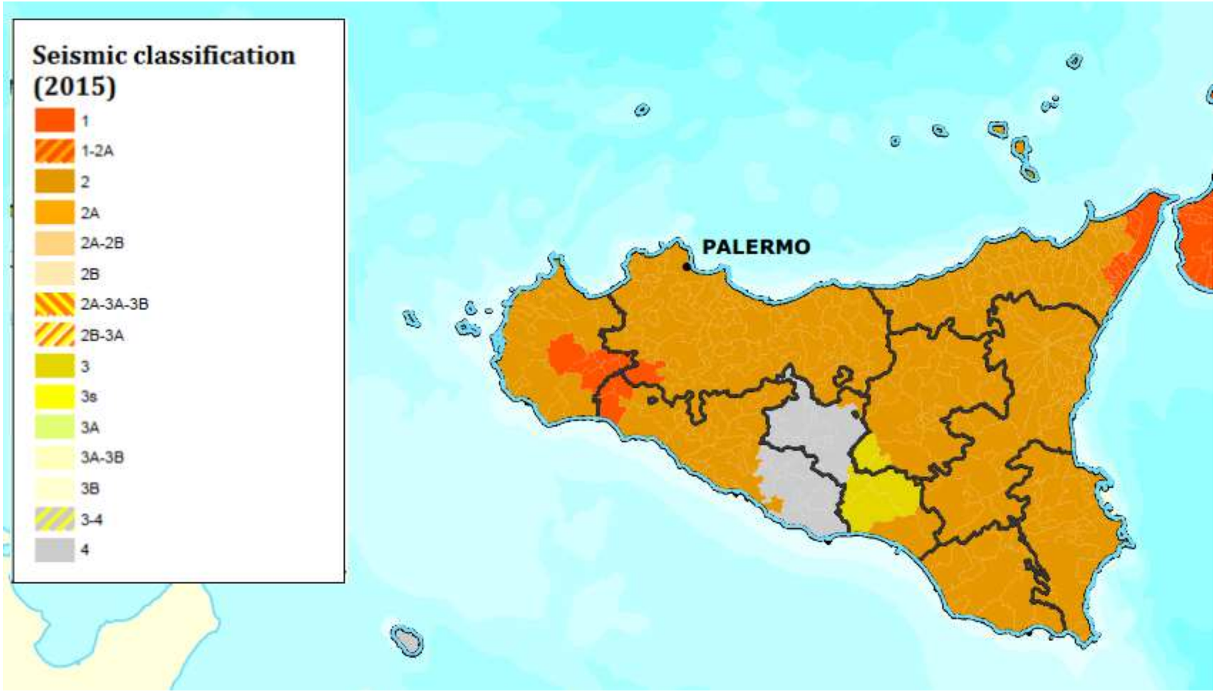

Figure 4.10. *Seismic classification (2015) of Sicily.*

According to this classification, the area of Priolo Gargallo is classified as level 2A.
Regarding Mount Etna, it’s about 90 km far from Priolo Gargallo, so there aren’t problems with lava flow during eruptions but there could be problems with ash fallout.
Volcanic ashes are small magma particles, of less than 2 mm in diameter, which are emitted into the atmosphere, cooled and consolidated, during an eruption. They are composed mainly of silicates and therefore are extremely abrasive. Volcanic ashes are particularly insidious due to the difficulty to be seen. In fact, in case of cloud cover, dark night, or simply when dilute (eg at a certain distance from the point of emission), they are hardly distinguishable from the normal atmospheric clouds. Since volcanic ash can also cause extreme danger to aircraft, abrasion to the fuselage and engine failure, the Civil Protection Department, with the National Authority for Civil Aviation - ENAC, the National Assistance Flight Board - ENAV, the Italian Air Force and the National Institute of Geophysics and Volcanology – INGV, has developed procedures looking to provide daily maps of areas potentially affected by the scattering of ashes, and to allow, in case of eruption, the immediate warning of air traffic controllers. Based on these daily procedures, prediction of wind fields for the next 48 hours is given to INGV in Catania and then INGV inserts the data into mathematical models of forecasting simulation taking into account the characteristics of a typical column of Etna ash: height, mass and volume erupted, temperature, particle size, etc.., forecasting and process maps.
INGV publishes these maps in its website so it’s possible to check if the area of Priolo Gargallo is interested in ash fallout or not.

In Figure 4.11a it’s shown the deposit load of ashes when Etna isn’t in activity, while in Figure 4.11b it’s shown the deposit load of ashes during an eruption of Etna. It’s clear that the deposit load of ashes in Priolo is low, so this feature will not be taken into account as possible risk.

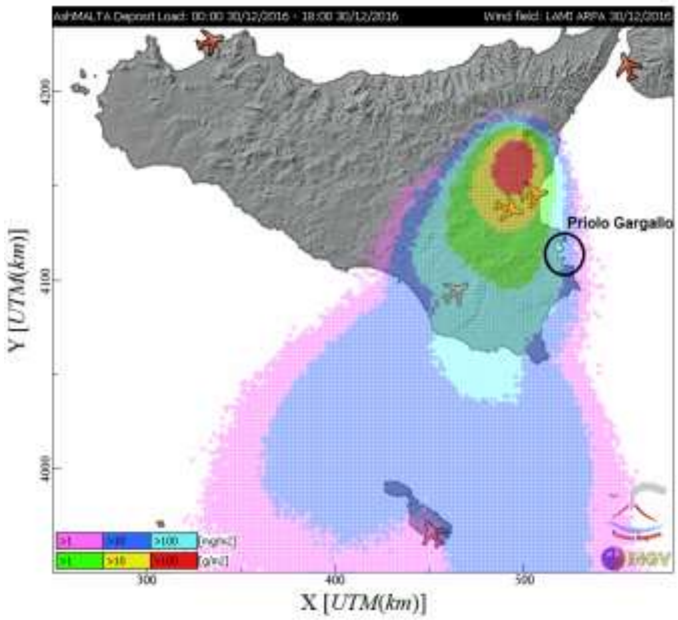

Figure 4.11a. *Deposit load of volcanic ashes without eruption of Etna.*

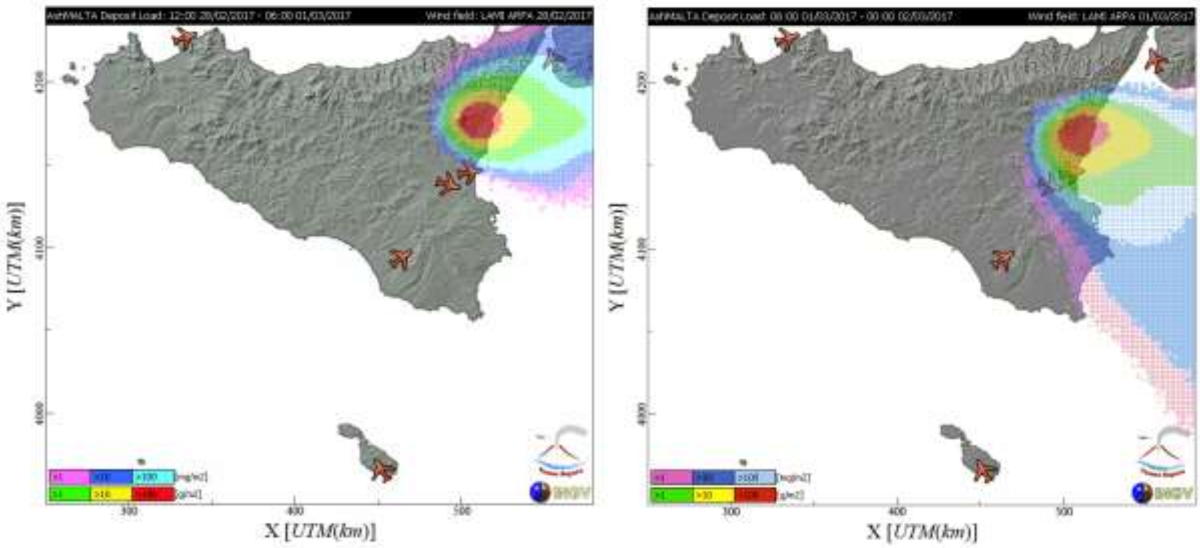

Figure 4.11b. *Deposit load of volcanic ashes with eruption of Etna.*

Another important natural event is rainfall, but precipitations in Sicily are low. In the report of 2008 of Hydrologic Risk of Sicily, it’s written that precipitations levels are within some ranges (around 1100 mm per year in the mountains areas and around 500 mm per year in the coastal areas) and they can be seen in Figure 4.12.

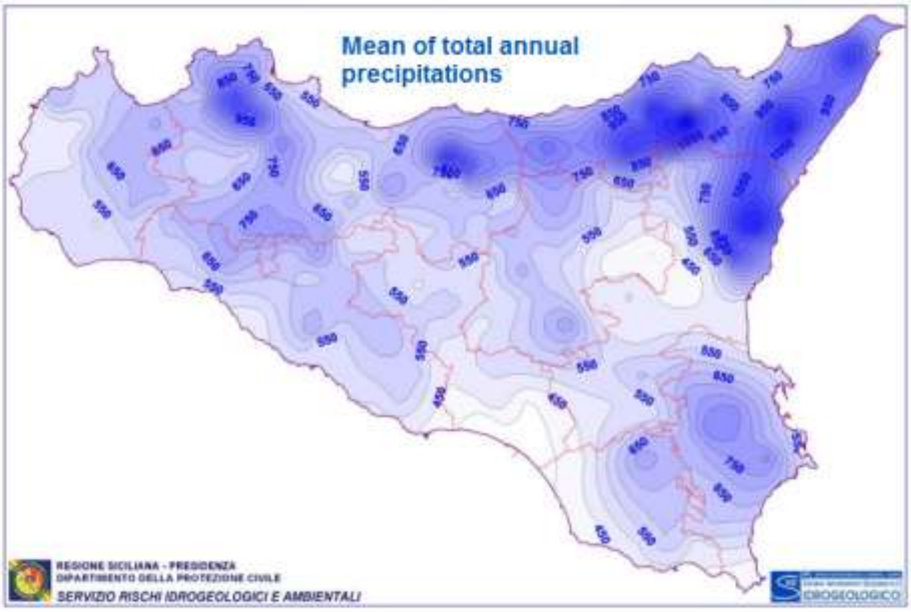

Figure 4.12. *Mean of total annual precipitations in Sicily.*

Furthermore, Sicily becomes more arid every year, as can be seen in Figure 4.13.
The different colours of Figure 4.13 are defined by the Crowther index, that is calculated as:

$$IC = P - 3{,}3 \cdot T$$

where P is the total annual precipitation (in cm) and T is the temperature (in °C).

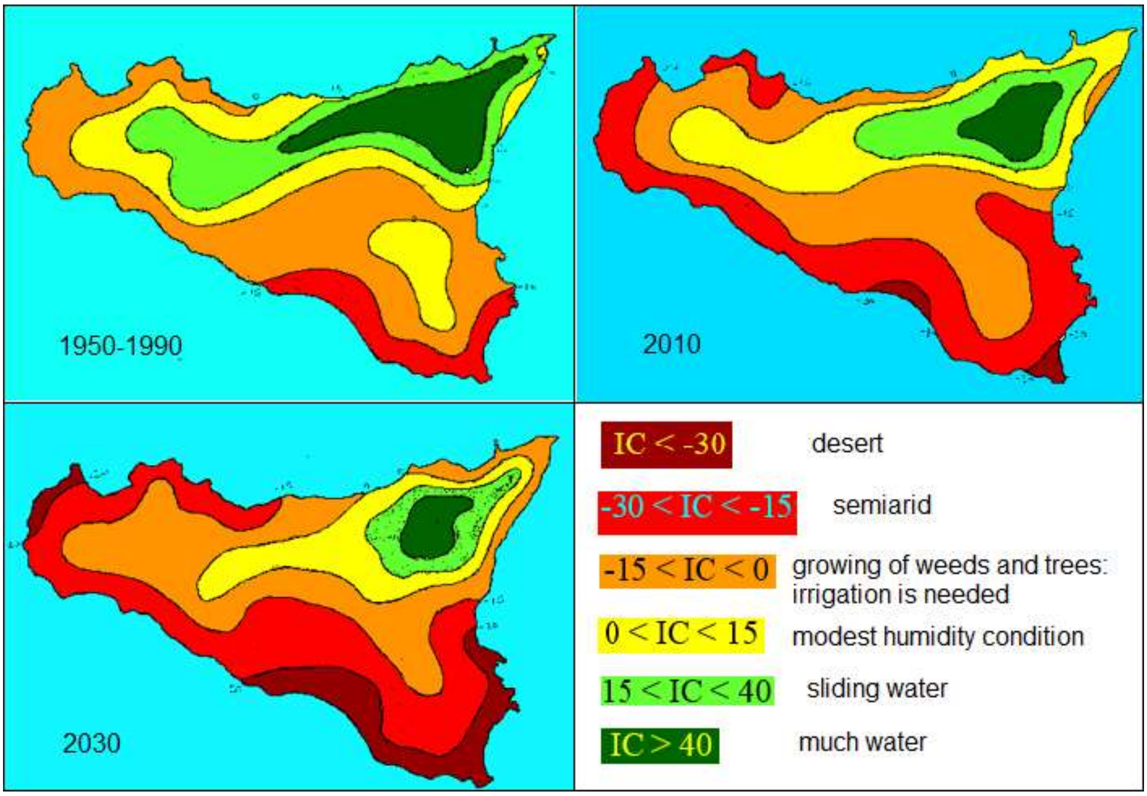

Figure 4.13. *Desertification of Sicily and legend of the Crowther index.*

Finally, regarding the lightning activity, it can be seen in Figure 4.7 that Sicily, in opposition of Veneto, is one of the region less affected by lightning.

4.3 Application of the DyPASI analysis

As explained in Chapter 3, the DyPASI analysis is composed by five steps:

0) Bow-tie analysis
1) Retrieval of risk notions
2) Prioritization
3) Atypical scenarios identification
4) Definition of safety measures

At this point all the information are available, thus the analysis can be started.

4.3.1 Bow-tie analysis

It's given the bow-tie for the green diesel release and it's shown in Figure 4.14.

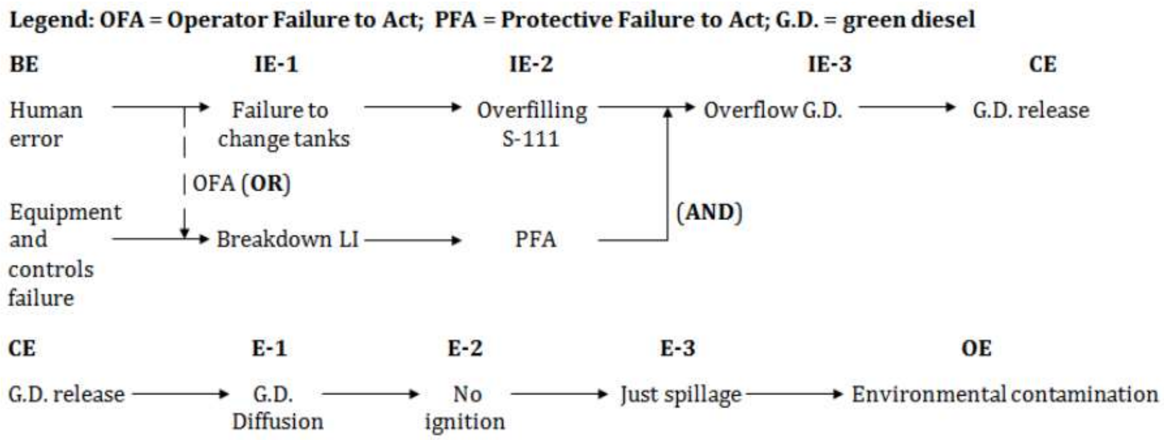

Figure 4.14. *Bow-tie for the top event green diesel release.*

The basic events (BEs) are two:

- the human error, due to the absence of action to change the tank after the signals indication of high level;
- the failure of equipment and controls, as the level indicator (LI, identification number not available) that causes the PFA.

The critical event (CE) has as unique direct consequence: the diffusion of liquid green diesel. Because it is supposed the elimination of ignition sources for the presence of ATEX areas where the S-111 is located, it's supposed the absence of ignition; the E-3 is only the green diesel spillage that can cause an environmental contamination of water and soil (water contamination can cause damages for the aquatic belief system).

4.3.2 Retrieval of risk notions

In this step, it's performed a search to find out undetected potential hazards that were ignored in conventional bow-tie development.

Some search systems are used to fulfil the research and are listed in the Table 4.1. It is impossible to use other important database as FACTS (Failure and Accidents Technical information System) and IChemE (Institution of Chemical Engineers) because, even if information of quality is present in their sites, they are not available in the open free version.

Table 4.1. *Search systems used for the retrieval of risk notions step.*

Search system	Information type
eNATECH (**Na**tural hazard-triggered **tech**nological accidents)	NaTech accident database
ARIA (Lessons learnt from industrial accidents)	Database opened by the French Ministry of Ecology, Sustainable Development and Energy
JST Failure Knowledge Database	Open reference sources on accidents and failures in science and technology field

It's necessary to highlight a limitation in the research using eNATECH, whose aim is to systematically collect worldwide Natech accidents and allow the searching and analysis of Natech accident reports for lessons-learning purposes. Since it's a new database, in fact it's opened after recent major natural disasters (such as the 2002 summer floods in Europe or Hurricanes Katrina and Rita in the United States in 2005), data of several accidents are not still published in the web-site, so the research is necessarily limited to the information with available data. In Tables 4.2 and 4.3 the research results about Natech events are reported, in particular in Table 4.2 there are accidents due to earthquakes, while in Table 4.3 accidents due to heavy rainfalls and lightning are listed. In the Tables, it's specified the location of the accident (the name of the company - when known -, the city and the nation), when it happens (day, month and year), some details about the accident (such as the causes, the sequence of events and the consequences) and the database from which the accident is found.

Table 4.2. *Research results about Natech events (earthquakes).*

Location	Date	Accident details	Database
Refinery of Showa Oil Co. - Niigata, Japan	16/06/1964	An earthquake (magnitude 7.5) caused the fire of five crude oil storage tanks: the cause of the fire was ignition by sparks generated by the collision of the floating roof with the side wall, which in turn was caused by the movement of the crude oil by the sloshing phenomenon. The fire also spread to two spherical tanks for LPG resulted in the splitting and buckling of a supporting leg. No injured, 286 houses were destroyed by the fire.	JST (EARTHQUAKE)
Refinery - Sendai, Miyagi, Japan	12/06/1978	An earthquake (magnitude 7.4) damaged seriously three storage tanks containing fuel oil. A crack was generated in the annular plate of a tank, the oil flowed out, washed away the foundation in front of a crack, and the crack expanded. Age deterioration of the annular plate was also one of causes. Environmental impacts: 68100 kL of fuel oil in the tank flowed out into the sea.	JST (EARTHQUAKE)
TUPRAS Izmit Refinery - Kocaeli, Turkey	17/08/1999	An earthquake (magnitude 7.4) ignited the naphtha in a naphtha tank farm because of the bouncing of the floating roof against the inner side of the tanks. No injured but economic losses.	eNATECH (EARTHQUAKE)
Refinery - Tomakomai, Hokkaido, Japan	26/09/2003	An earthquake (magnitude 8) caused damages at the floating roof of a naphtha tank; the roof sank, naphtha floated above the roof and ignited. Environmental impacts, physical discomforts accused by several people and economic losses.	JST (EARTHQUAKE)
Cosmo oil Refinery -Tohoku, Japan	11/03/2011	An earthquake (magnitude 9) caused damages on the LPG tank legs that provoked the LPG tank collapse and LPG pipes severing and leakage; there were fire and explosion. There were several injured, a little environmental impact for and economic losses.	eNATECH (EARTHQUAKE)

Table 4.3. *Research results about Natech events (heavy rainfalls and lightning).*

Location	Date	Accident details	Database
Refinery - Kurashiki, Okayama, Japan	17/10/1987	Due to a heavy rainfall, which continued for more than 1 hour 30 minutes, the floating roof sank into the naphtha. A large amount of rainwater remained on the roof because the roof drain sump mouth was blocked with dust. Water got into two pontoons because someone forgot to close the cap of the nozzle for airtight tests of the pontoon. An abnormal load was put on the roof and it sank into the naphtha.	JST (HEAVY RAINFALL)
Pertamina Cilacap Refinery - Indonesia	24/10/1995	A lightning struck the automatic gauge device of an oil tank with a consequential sparks production (for poor equipotentiality) and oil ignition; the burning liquid ran over other naphtha tanks (domino effect). No injured but economic losses.	eNATECH (LIGHTNING)
Refinery - Kawasaki, Kanagawa, Japan	30/09/1998	A large amount of rainwater fell into a high-temperature flange due to the failure of heat insulation causing a contraction of the material; hydrogen and gas oil mist leaked and ignited. Few economic losses.	JST (HEAVY RAINFALL)
Samir Mohammedia Refinery -Morocco	25/11/2002	The large amount of rainwater caused the collapse of a storage tank roof with gas, vapour and oil releases that were ignited and then deflagrated. There were several fatalities and injured, economic losses and also community disruption.	eNATECH (HEAVY RAINFALL)
Refinery - Feyzin, France	17/09/2011	A lightning struck a water tank contained some hydrocarbon amounts and caused the tank ignition and the opening along the weakest weld. Environmental contamination.	ARIA (LIGHTNING)

Tables 4.2 and 4.3 are reports of the collected events for which there were enough data, for example, regarding earthquakes, in the eNATECH database there is a list of events, but data have not been published yet.

4.3.3 Prioritization

With the previous step, several data and information are obtained, thus, to go further, it’s important to understand whether the data are significant enough to trigger further action and proceed with the process of risk assessment. As a support of this process of prioritization (step 2 of DyPASI application), a register collecting the risk notions obtained from the retrieval process and showing their relative relevance and impact can be obtained. Possible consequences can be determined based on the risk notions and ranked by means of the following scale of severity levels (as defined in Chapter 3): 1-*Near miss*, 2-*Mishap*, 3-*Incident*, 4-*Accident*, 5-*Disaster*.

Adopting this classification, in Tables 4.4 and 4.5 the events above-mentioned in Table 4.2 and 4.3 are listed on the base of cause typology and prioritized.

Table 4.4. *Prioritization of collected data from the research of Table 4.2.*

Cause and event typology	Date	Consequences	Severity
Natech (Earthquake)	16/06/1964	- scenario: fire (unknown type) and liquefaction of the ground - casualties: no - community disruption: 286 of house was destructed by fire - environmental impact: unknown - economic losses: unknown	MISHAP
NaTech (Earthquake)	12/06/1978	- scenario: outflow of all fuel oil from a tank - casualties: no - community disruption: unknown - environmental impact: 68100 kL of fuel oil flowed into the sea - economic losses: unknown	INCIDENT
NaTech (Earthquake)	17/08/1999	- scenario: pool fire - casualties: no - community disruption: industrial areas, residential areas, commercial areas, public areas, infrastructure. Train services connecting Ankara and Istanbul were disrupted because of the fire - environmental impact: large quantities of oily water flooded the wastewater treatment plant, and subsequently flowed into the Izmit Bay - economic losses: 57800 thousand USD	INCIDENT
NaTech (Earthquake)	26/09/2003	- scenario: fire (unknown type, maybe jet fire) - casualties: no - community disruption: people physical discomfort - environmental impact: high concentration of carcinogenic substances - economic losses: shut down for 43 hours and 81393 thousand USD	INCIDENT
NaTech (Earthquake)	11/03/2011	- scenario: fireball and UVCE/VCE - casualties: 6 injured (1 major injured) - community disruption: contamination of water by material (was recovered but more data are not available) - environmental impact: high concentration of carcinogenic substances - economic losses: heavy damages in-site and out-site the refinery	ACCIDENT

Table 4.5. *Prioritization of collected data from the research of Table 4.3.*

Cause and event typology	Date	Consequences	Severity
NaTech (Heavy Rainfall)	17/10/1987	- scenario: rupture of a floating roof tank and release of naphtha - casualties: no - community disruption: no - environmental impact: no - economic losses: unknown	NEAR MISS
NaTech (Lightning)	24/10/1995	- scenario: tank fire and explosion (unknown type) - scenario: pool fire as domino effect (the liquid naphtha spread fire to other 6 tanks) - casualties: no - community disruption: damages to residential areas - environment impact: contamination of water bodies - economic losses: yes, for business interruption	INCIDENT
NaTech (Heavy Rainfall)	30/09/1998	- scenario: fire (unknown type, maybe a jet fire) - casualties: no - community disruption: no - environmental impact: no - economic losses: yes, of minor entity	MISHAP
NaTech (Heavy Rainfall)	25/11/2002	- scenario: vapour release, fire and explosion (UVCE/VCE) - casualties: 2 fatalities and 4 injured - community disruption: yes, for the necessity to buy fuels from international markets - environmental impact: no - economic losses: damages for 200000 thousand USD and shut down of the plant for 9-13 months	DISASTER
NaTech (Lightning)	19/07/2011	- scenario: tank fire - casualties: no - community disruption: unknown - environment impact: Rhone river canal contamination with foam - economic losses: unknown	MISHAP

For the evaluation of the events severity, there are several events that can fall in more than one category: in these cases, it is given more importance to the human health (if there are or not casualties), then the environment damages are considered (possible water, air and soil contamination) and only as last aspect the economic and property costs are taken into account.

4.3.4. Atypical scenarios identification

The third step is focused on the identification of atypical scenarios. As described in Chapter 3, the identification has a qualitative approach, based on the historical analysis on past events, but it’s possible to have no consequences for the low amount of the released substance or for other reasons. Nevertheless, it’s equally important to identify atypical scenarios previously neglected to evaluate them and conclude that they can be ignored only after their examination. The

procedure suggested by DyPASI is the *Why Tree* technique. The first thing to do is to identify the BE, the CE and the OE within the potential atypical scenario. Then, starting from OE and going backward through CE until BE, the other elements are defined asking questions, such as "why?". The integration of the atypical scenario pattern should be performed considering one half of the diagram at a time.
The top event is the green diesel release due to an overflow from the storage S-111.
At this point it’s necessary to update the bow-tie for Porto Marghera plant and for Priolo Gargallo plant separately, according to the different vulnerability of the areas.

4.3.4.1. Porto Marghera bow-tie

First, it's considered the left side of the bow-tie diagram and it's possible to identify a new BE: the NaTech. Due to the NaTech events, in Porto Marghera plant two Intermediate Events (IE-1s) are defined: the earthquake and the heavy rainfall. For the former, IE-2 and IE-3 are the mechanical stress and then the collapse of the equipment. In fact, considering the event happened the 26th September 2003 reported in Table 4.2, the sinking of the roof could cause the green diesel release; for the latter, IE-2 and IE-3 are the insufficient mechanical properties of the tank and the consequent collapse of the storage tank. In fact, according to the event in Table 4.3 dated 25th November 2002, the storage tank roof collapsed due to the large amount of rainwater.
At this point, it's necessary to consider the other half part of the bow-tie diagram. Adopting the classical procedure, no ignition is considered due to the presence of ATEX areas where the S-111 is located. But, considering the data obtained in the previous steps it's possible to build a new event tree because of atypical ignition sources:

- the lightning strike is one of the most likely ignition sources, as shown in Figures 4.7 and 4.8 and also reported in Table 4.3 with the events happened in the 24th October 1995 and the 17th September 2011;
- the earthquake (already identified as intermediate event in the left half of the bow-tie) can be also the cause of the flammable substances ignition due to the bouncing of the floating roof against the inner side of the tank, as described in Table 4.2 with the past events dated 16th June 1964 and 17th August 1999.

So, the modified event tree is shown in Figure 4.12, where the probability of occurrence was calculated in a previous work.
The continuous liquid release of green diesel has as more likely scenario the spillage (that is indeed the unique scenario identified with the conventional hazard identification procedure). In addition, there are other three scenarios: a pool fire, a flash fire and a UVCE/VCE.

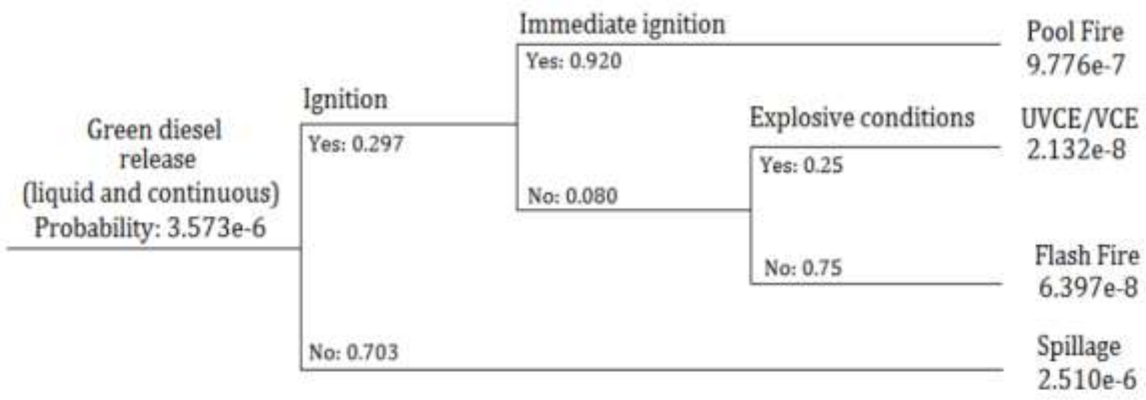

Figure 4.12. *Modified event tree.*

Now, it's possible to draw the integrated bow-tie, considering the modifications (drawn in blue) to both parts of the diagram and it's shown in Figure 4.13a and 4.13b.

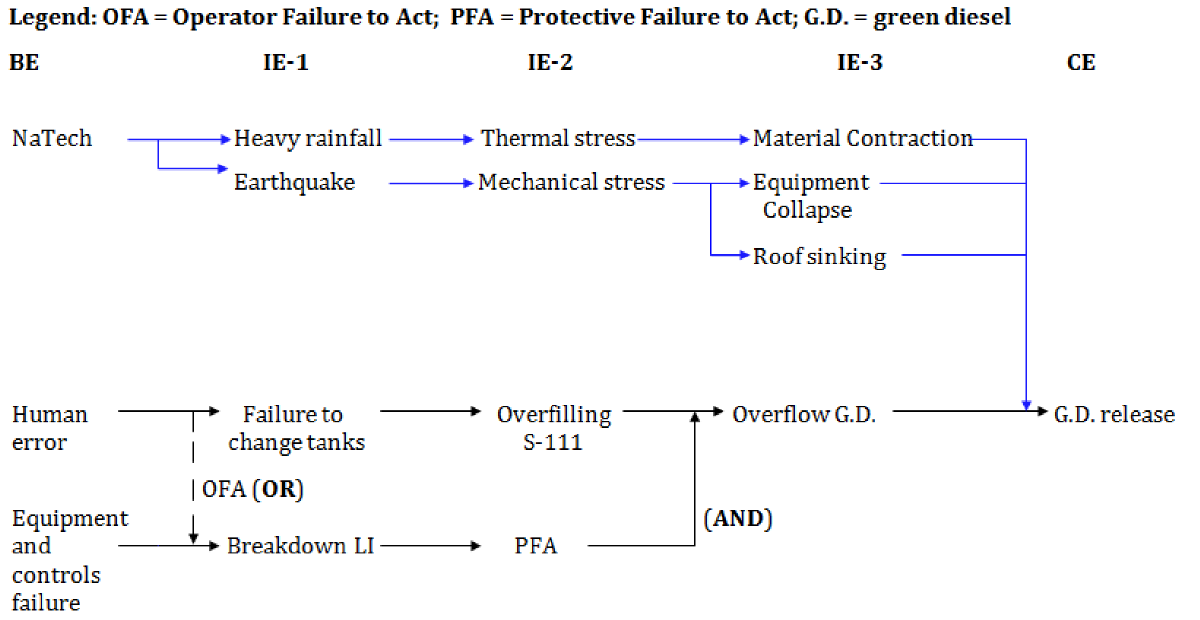

Figure 4.13a. *Graphic representation of the left-hand bow-tie of the plant located in Porto Marghera.*

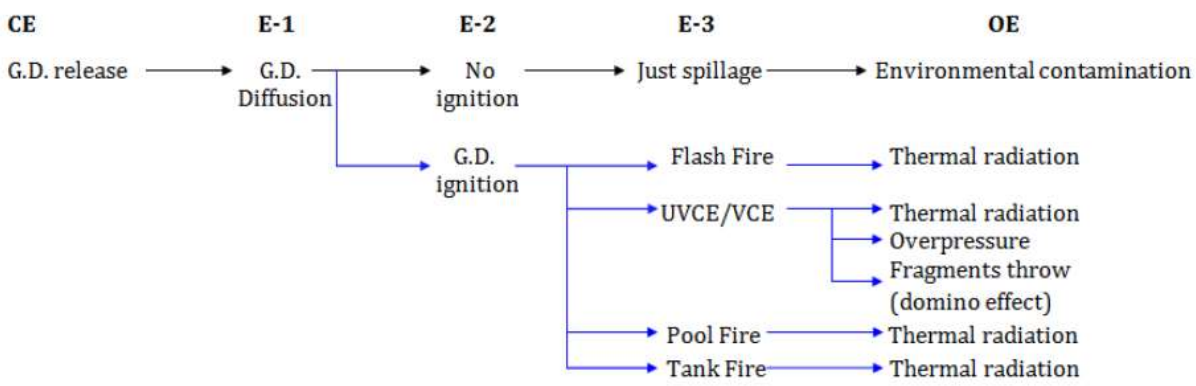

Figure 4.13b. *Graphic representation of the right-hand bow-tie of the plant located in Porto Marghera.*

4.3.4.2. Priolo Gargallo bow-tie

Even in this case it's considered first the left part of the bow-tie and the new BE is the NaTech. Due to the NaTech events, in Priolo Gargallo plant the Intermediate Event (IE) is the earthquake and IE-2 and IE-3 are, as for Porto Marghera plant, the mechanical stress and then the collapse of the equipment, considering, as before, the event happened the 26th September 2003 reported in Table 4.2 (sinking of the roof that could cause the green diesel release).

Regarding the right part of the bow-tie, since it's possible to identify an atypical ignition source, that is the earthquake, the event tree is modified as in the previous paragraph (Figure 4.12). In fact, as reported in Table 4.2, earthquake could be the cause of the ignition of flammable substances due to the bouncing of the floating roof against the inner side of the tank (events dated 16th June 1964 and 17th August 1999). In Figure 4.14a and 4.14b there are the left hand and right hand, respectively, of the bow-tie of the plant located in Priolo Gargallo.

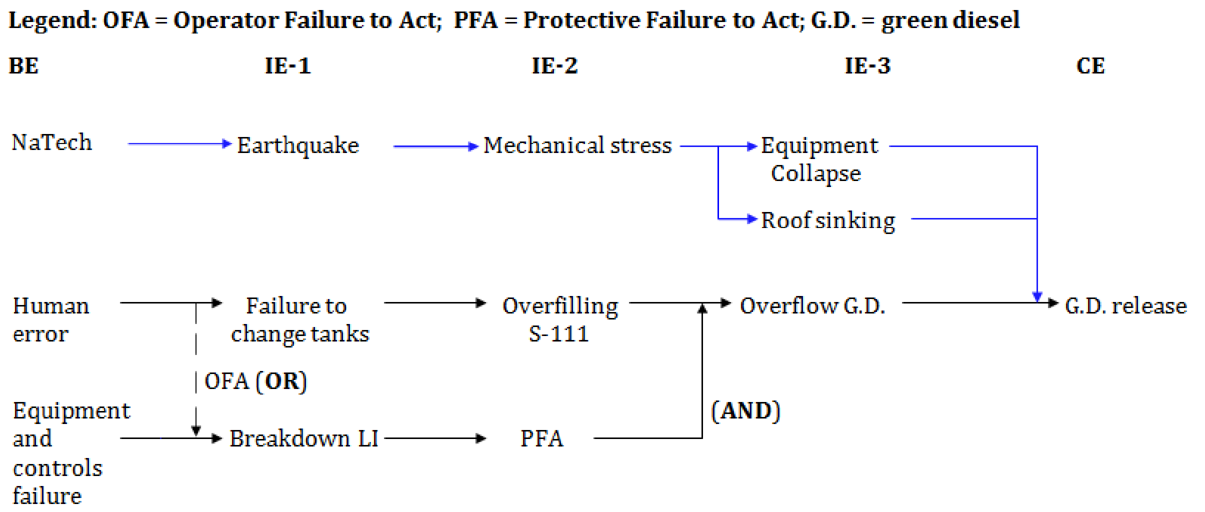

Figure 4.14a. *Graphic representation of the left-hand bow-tie of the plant located in Priolo Gargallo.*

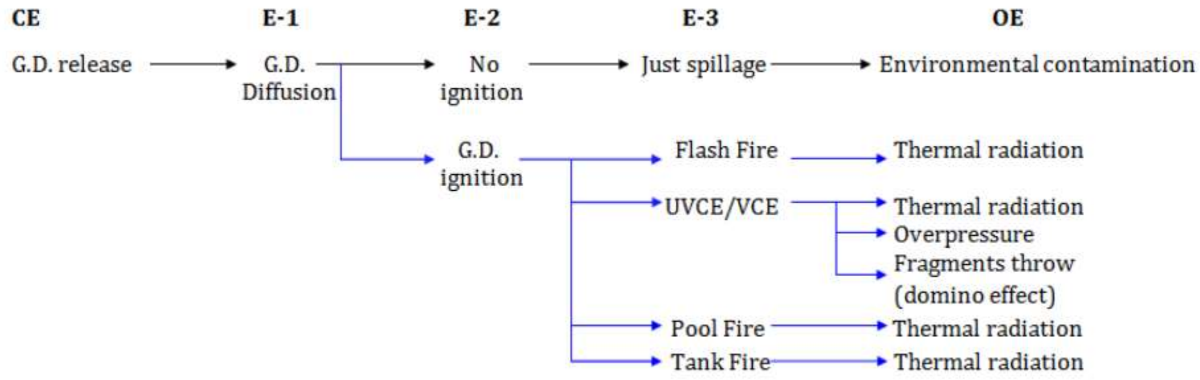

Figure 4.14b. *Graphic representation of the right-hand bow-tie of the plant located in Priolo Gargallo.*

Chapter 5

Fault tree analysis: procedure and numerics

In the previous chapter, the bow-ties, for the cases of the plant located in Porto Marghera and in Priolo Gargallo, were updated considering also the NaTech events. The following step is the Quantitative Risk Assessment in order to obtain the final frequency of the top event.
In this chapter, the procedure application is explained and part of the Matlab code used to perform the calculation is shown.

5.1 Probabilistic approach

As stated in Paragraph 3.3, the Quantitative Risk Assessment is a deterministic approach that allows to estimate the failure frequency values, once the potentially hazardous events are identified. But, considering also the seismic risk, the deterministic approach often leads to an overestimation of the risk. So, a risk assessment that comprehend both mechanical and seismic risk has to be written using the probabilistic approach. Whereas for a simple chemical risk assessment based on mechanical failure the deterministic model fits well, in a seismic analysis, which is based on the probability of the PGA to exceed the seismic capacity of a tank, only a probabilistic model can generate a good report.

5.2 Data conversion

The chosen method is the probabilistic one but failure frequencies are presented as numbers and not with their probabilistic distribution.
In order to use failure frequency in the system, it is important to convert these values properly. The values that need to be transformed are the mechanical failure frequency and the frequency associated to heavy rainfalls, since they are expressed in a deterministic way. The overflow of the green diesel has a frequency of $3{,}573 \cdot 10^{-6}$ events/year, this number is extracted by the Eni N.A.R. report (2013). While the failure frequency related to heavy rainfalls is about 0,2353 events/year. This value has been calculated from a report of Veneto regional council (2012), in which there is a list of the worst climatic events.

Thus, these events are characterized by a constant failure rate λ and the probability distribution to be used is the exponential one.
The probability density function of the exponential distribution is expressed by Equation (5.1):

$$f(t) = \lambda e^{-\lambda t} \quad (5.1)$$

The exponential distribution is frequently used in reliability and safety studies. The distribution is characterized by a constant failure rate and a constant mean time to failure. Another characteristic of the exponential distribution is that the probability of failure in the interval (t, t+Δt) is the same as the probability of failure in any interval of the same length, given that no failure has occurred up to time t.

5.3 Procedure application

The first step of the probabilistic fault tree analysis is the identification of the fault tree logic scheme, which was developed in Chapter 4 for the cases of the plant located in Porto Marghera and in Priolo Gargallo. In Figure 5.1 there are the two fault trees.

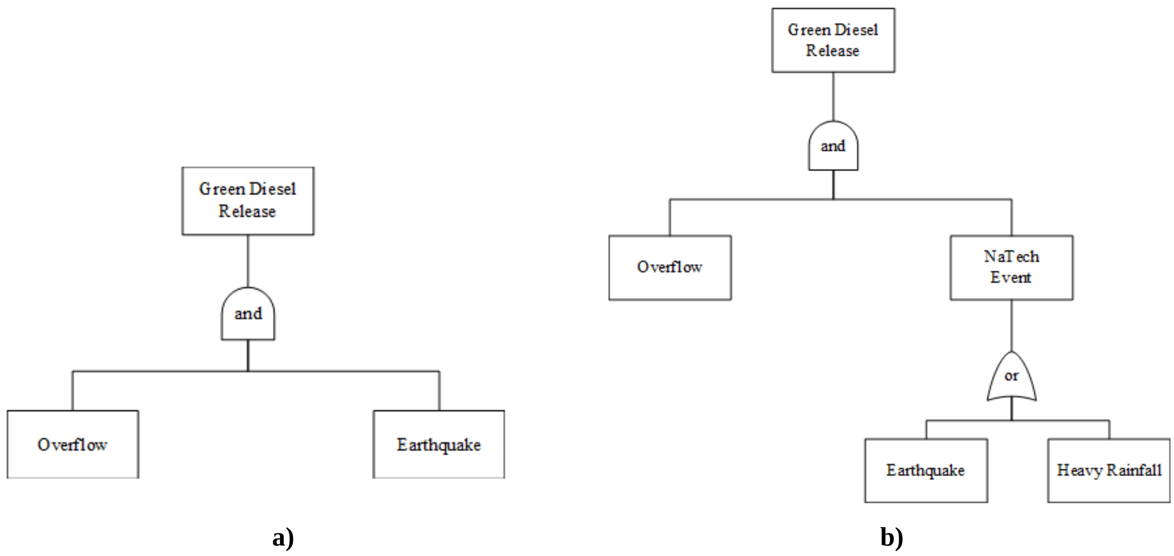

Figure 5.1. *Part a) is the fault tree of the plant located in Priolo, while part b) is the fault tree of the plant located in Porto Marghera.*

The seismic hazard curve, for both cases (Porto Marghera and Priolo Gargallo), is retrieved from the Italian Institute of Geophysics and Volcanology (INGV) with reference to the 10% in 50 years PGA hazard map.
Data collected from INGV are presented in paragraph 5.3.1 and 5.3.2.

5.3.1 Porto Marghera

In Figure 5.2 it's shown the map of the area of Porto Marghera in terms of possible values of PGA.

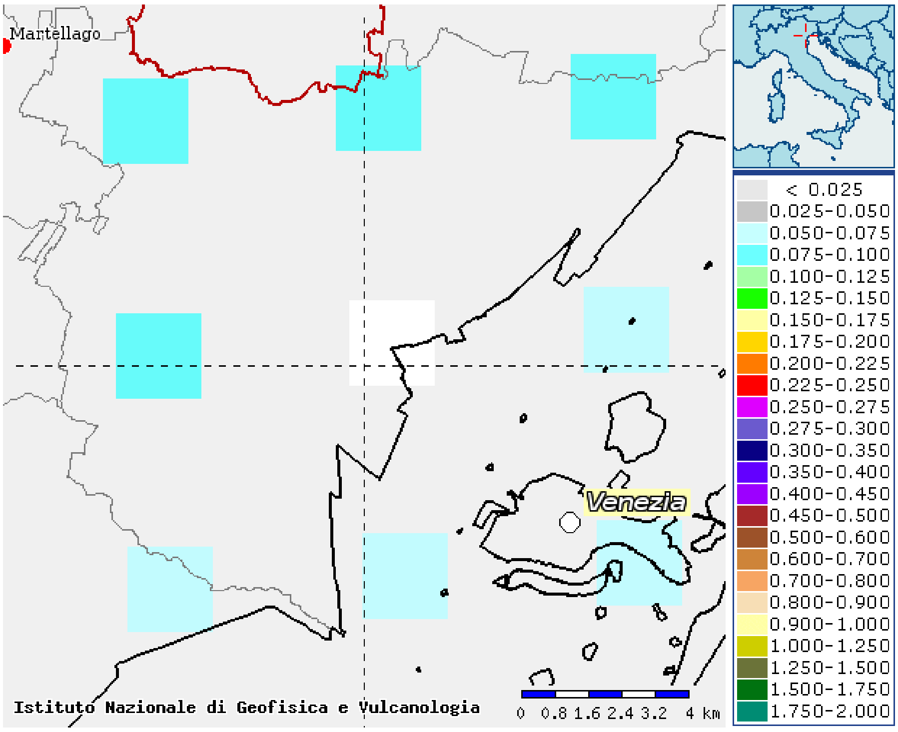

Figure 5.2. *Seismic map of Porto Marghera. Possible PGAs in case of earthquake are represented in coloured squares. On the right, the legend presents the scale: the area is subject to earthquake with PGAs from 0.05g to 0.100g.*

With this map, the INGV gives also a table concerning the probability of a seismic event, sorted by the distance and the magnitude. The values are reported in Table 5.1.

With this table, it's possible to note the couples of M (magnitude) and R (distance) values representative of the earthquake mostly contributing to the seismic hazard of the site of interest. In this case, the tank is influenced by earthquakes with epicentre between 30 and 170 km far from its location. These earthquakes have magnitude that can vary from the fourth and the seventh degree of the Richter's scale.

Table 5.1. *Probabilities of an earthquake in Porto Marghera, sorted by magnitude in Richter scale (in the columns) and distance (in the rows) from the epicentre. The value of these quantities is the mean of border values of the interval.*

distance (km)	Magnitude					
	4,25	**4,75**	**5,25**	**5,75**	**6,25**	**6,75**
35	2,11	7,13	8,28	7,44	5,36	0,796
45	1,05	4,88	6,89	7,13	5,82	0,932
55	0,116	2,13	4,24	5,15	4,79	0,826
65	0	0,61	2,43	3,55	3,73	0,69
75	0	0,066	0,965	1,81	2,17	0,428
85	0	0	0,352	1,03	1,28	0,263
95	0	0	0,119	0,671	0,866	0,183
105	0	0	0,026	0,51	0,824	0,188
115	0	0	0	0,3	0,636	0,154
125	0	0	0	0,129	0,403	0,104
135	0	0	0	0,041	0,218	0,061
145	0	0	0	0,007	0,075	0,023
155	0	0	0	0	0,011	0,003
165	0	0	0	0	0,002	0

A last consideration for seismic risk is the presence of a frequency factor: it represents the frequency of return of an earthquake with a chosen magnitude. The calculation of this vector can be performed using the Equation (5.1):

$$f_m = \frac{10^{(a-bM)}}{50} \tag{5.1}$$

This equation highlights the frequency dependence upon three parameters: *a* and *b* are constants derived by seismic analysis of the area, while M represents the magnitude of the earthquake as in Table 5.1. It is worth to be noticed the parameter 1/50: it represents the return period considered by INGV in the calculation of the earthquake matrix.

In order to obtain parameters *a* and *b*, it's necessary to look at the map of the seismogenic zonation of Italy, that it's shown in Figure 5.3, and identify the area in which the plant is located. Once the area is selected, there's a table in which it's possible to choose *b* parameter, while the parameter *a* is fixed and it's equal to 4,76 per each area, except in zone ZS 936 (Etna), where *a* is equal to 4,30.

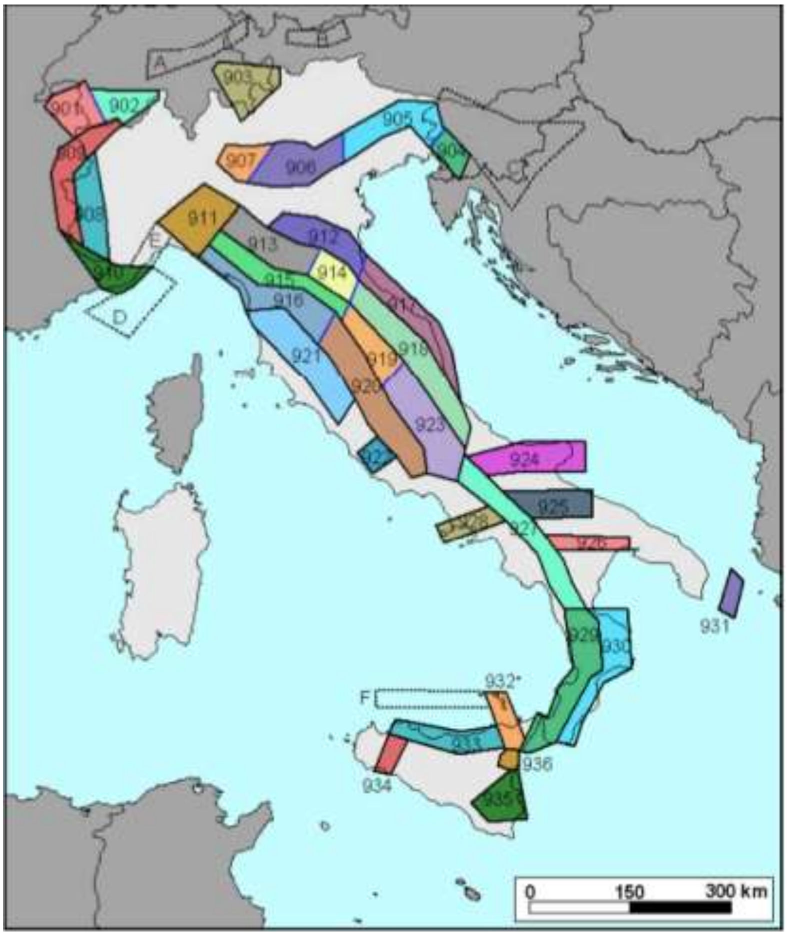

Figure 5.3. *Seismogenic zonation of Italy (ZS9), for frequency calculation.*

As can be seen in Figure 5.3, Porto Marghera isn't identified by a specific area, for this reason the calculation of the frequency is achieved using the parameters of the following areas: Friuli – Veneto orientale (905), Garda – Veronese (906) and Dorsale Ferrarese (912) that are the closest to the point of interest. Then, in the next calculations, only the maximum and minimum frequencies will be considered.

In Table 5.2 there are the results of the calculation of the frequency per each area considered.

Table 5.2. *Frequency vector with the parameter of the three areas (Friuli, Garda and Dorsale Ferrarese).*

		Magnitude					
		4,25	**4,75**	**5,25**	**5,75**	**6,25**	**6,75**
ZS	**b**	**Frequency**					
905	**1,06**	0,035977	0,010617689	0,003134	0,000925	0,000273	8,05E-05
906	**1,14**	0,016445	0,004426189	0,001191	0,000321	8,63E-05	2,32E-05
912	**1,35**	0,002106	0,000445174	9,41E-05	1,99E-05	4,2E-06	8,88E-07

Looking at Table 5.2, it's possible to highlight that the area with the maximum frequency is the Friuli one, while Dorsale Ferrarese has the minimum frequency. Thus, calculations will be performed with these two frequencies.

5.3.2 Priolo Gargallo

Figure 5.4 represents the map of the area of Priolo Gargallo in terms of possible values of PGA.

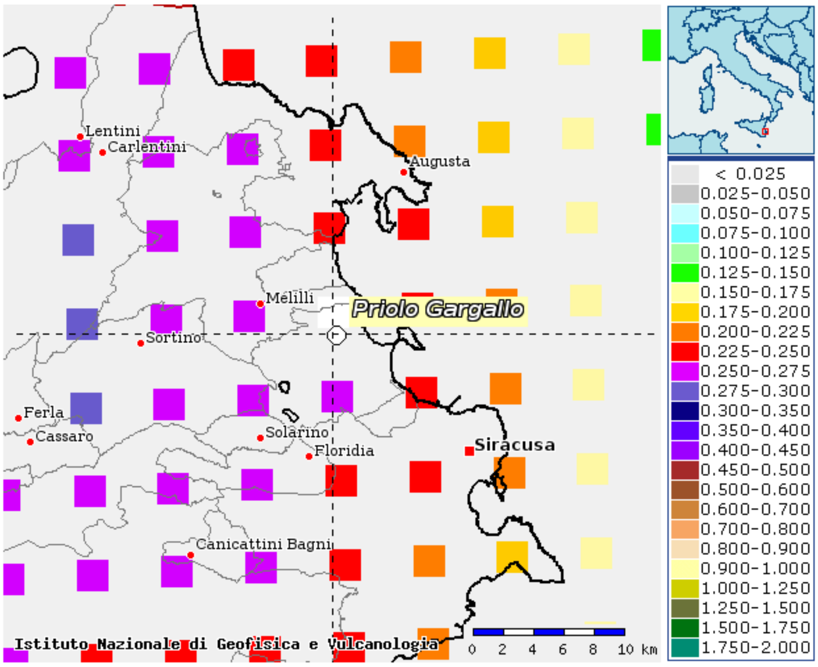

Figure 5.4. *Seismic map of Priolo Gargallo. Possible PGAs in case of earthquake are represented in coloured squares. On the right, the legend presents the scale: the area is subject to earthquake with PGAs from 0.150g to 0.300g.*

It's possible to see that this area has a seismic risk that is much higher than the previous case. Table 5.3 collects the probability of a seismic event, sorted by the distance and the magnitude.

Table 5.3. *Probabilities of an earthquake in Priolo Gargallo, sorted by magnitude in Richter scale (in the columns) and distance (in the rows) from the epicentre. The value of these quantities is the mean of border values of the interval.*

distance (km)	Magnitude							
	4,25	**4,75**	**5,25**	**5,75**	**6,25**	**6,75**	**7,25**	**7,75**
5	3,58	11,4	13,5	13,4	11,2	8,03	5,08	0,726
15	0,037	0,579	1,92	3,67	5,16	5,76	5,25	0,912
25	0	0	0,036	0,448	1,24	2,12	2,74	0,578
35	0	0	0	0,01	0,21	0,605	1,04	0,253
45	0	0	0	0	0,011	0,112	0,266	0,073
55	0	0	0	0	0	0,014	0,062	0,019
65	0	0	0	0	0	0	0,006	0,002
75	0	0	0	0	0	0	0	0,001

The magnitude interval in this case comprehend also earthquake of the seventh degree of Richter's scale with peak of eighth. These huge earthquakes can be perceived from 80 km away from the epicentre. Compared with the previous case, the seismic risk associated with Priolo is much higher.
Regarding the frequency calculation, Priolo is situated in the area 935 of the map of Figure 5.2, and has the following parameters used in Equation (5.1):

- a=4,76;
- b=0,72.

The resulting vector is reported in Table 5.4.

Table 5.4. *Frequency vector of earthquake for Priolo (SR) sorted by magnitude.*

Magnitude	**4,25**	**4,75**	**5,25**	**5,75**	**6,25**	**6,75**	**7,25**	**7,75**
Frequency	1,002374	0,437552	0,190999	0,083374	0,036394	0,015887	0,006935	0,003027

5.3.3 GMPE and fragility functions

For each earthquake scenario characterized by a specific magnitude M, epicentre distance R and percent contribution to the seismic hazard of the site of interest, the PGA probability density function is derived using an updated version of the Sabetta and Pugliese of 1996 (SP96) that is the mostly used empirical Ground Motion Prediction Equation (GMPE) for Italy.
The SP96 functional form for PGA and PGV is defined in Equation (5.2):

$$\log_{10} y = a + bM + c \log_{10} \sqrt{R^2 + h^2} + e_i S_i \quad (5.2)$$

Where y is the response variable (maximum between horizontal components), M is the magnitude and R is either the epicentral or the Joyner-Boore distance in [km]; the PGA is measured in [cm/s^2] and the PGV in [cm/s]. Variables S_i are dummy variables which assume the 0/1 value depending on the site class (rock: S_0=1 and S_1=S_2=0; shallow alluvium: S_1=1 and S_0=S_2=0; deep alluvium: S_2=1 and S_0 =S_1=0).
Concerning the variable S_i, in both cases, of the plant located in Porto Marghera and in Priolo Gargallo, the site class chosen is the deep alluvium.
In Table 5.5 there are the values of the parameters that have been corrected from the SP96.

Table 5.5. *Values of the parameters of the GMPE.*

Parameter	**a**	**b**	**c**	**h**	**e_0**	**e_1**	**e_2**	**σ**
PGA	1,344	0,328	-1,09	5	0	0,262	0,096	0,32

Once disaggregated seismic hazard, the following step is the assessment of probabilities of detecting a certain damage state: in this thesis, the fragility functions for atmospheric steel tanks proposed by Salzano *et al.* (2003) and collected in Tables 1.2 and 1.3 were adopted for characterizing seismic vulnerability of the tank under analysis.

5.4 Numerics

The procedure described in the previous paragraph is developed in a Matlab code, in order to simulate all the possible PGAs in a seismic zone and to calculate as precisely as possible the value of the risk.
The program is formed by sections regarding the calculation of different aspects of the risk and then the last section that resume all risks using the fault tree analysis.

5.4.1 Seismic failure

The first section of the code concerns about the calculation of seismic risk. In order to resume how the calculation is performed, a part of the program is reported below.

```
R=xlsread('DistribuzioniPriolo.xlsx', 'distanza', 'A1:A8');
M=xlsread('DistribuzioniPriolo.xlsx', 'Magnitudo', 'A1:H1');
MP=xlsread('DistribuzioniPriolo.xlsx', 'matrice', 'A1:H8');
F=xlsread('DistribuzioniPriolo.xlsx', 'Frequenza', 'A1:H1');

r=length(R);
m=length(M);
logPGA=[];
for i=1:r
    for j=1:m
        logPGA(i,j)=1.344+0.328*M(j)-1.09*log10(sqrt(R(i)^2+5^2))+0.096;
    end
end

sigma=0.32;
mu2=0.3;
sigma2=0.6;
mu3=1.25;
sigma3=0.65;
PeqRS1=[];
PeqRS2=[];
PeqRS3=[];
PeqRS1=zeros(rand,1);
PeqRS2=zeros(rand,1);
PeqRS3=zeros(rand,1);

for i=1:rand
    PGA1=random ('norm',logPGA,sigma);
    PGA=(10.^PGA1)*9.81/100;
    RS3eq= cdf('logn',PGA,mu3,sigma3);
    RS2eq=cdf('logn',PGA,mu2,sigma2);
    Prs1=(1-RS2eq).*(MP./100);
```

```
    Prs2=(RS2eq-RS3eq).*(MP./100);
    Prs3=RS3eq.*(MP./100);
    PfRS11=sum(Prs1).*F;
    PfRS1=sum(PfRS11(:));
    PfRS22=sum(Prs2).*F;
    PfRS2=sum(PfRS22(:));
    PfRS33=sum(Prs3).*F;
    PfRS3=sum(PfRS33(:));
    PeqRS1(i)=[PfRS1 ];
    PeqRS2(i)=[PfRS2 ];
    PeqRS3(i)=[PfRS3 ];
    i=i+1;
end

PeqRS =[PeqRS1 PeqRS2 PeqRS3];
```

The first part uses data by the INGV, these values were collected in an Excel file divided in distances, magnitudes (both of them using the mean value of the interval considerate), frequencies and the matrix of possible probabilities.

Using a random value of distance and magnitude, it is possible to simulate an earthquake with a defined PGA, calculated and expressed in this case in logarithmic scale with the updated SP96. The next step concerns the calculation of the lognormal distribution of PGAs, before risk calculation.

It is important to know that there are three possibilities for a seismic impact in a plant, divided by the dimension of the leakage. To obtain a precise representation, all possibilities have to be examined.

Next step defines three vectors, one for each failure severity. Then, calculating the cumulative distribution function using lognormal and parameters, it is possible to achieve a result expressed by a matrix of seismic risk.

5.4.2 Mechanical failure

The second section of the code concerns about the calculation of mechanical failure. Part of the program is reported below.

```
lambda=3.573E-6;
time=50;
t=[0:0.1:time];
f=lambda*exp(-lambda.*time);
X=[];

for i=1:rand
    X(i)=random ('exp',f);
    RS(i)=X(i);
end

RS=RS';
PmRS=RS;
```

As said in Par 5.2, since it's given only a deterministic value of the failure frequency, it's used the exponential distribution to convert this value. Then, random values of the probability distribution function are generated. Here it's considered only one value of the release state, in such way it's avoided to count twice the division of the release states done by LNE Department, since the final function is obtained multiplying the seismic risk matrix with the mechanical failure probability.

5.4.3 Heavy rainfall failure

This section, concerning the calculation of the probability of failure due to heavy rainfalls, it's only present in the code of the atmospheric steel tank located in Porto Marghera, as a result of the vulnerability analysis done in Paragraph 4.2.1. As in the case of the mechanical components failure, there is only a value of the failure frequency. Thus, it's used the exponential distribution to convert the value and below part of the program is shown.

```
lambda_rain=0.2353;
time=50;
f_rain=lambda_rain*exp(-lambda_rain.*time);
X_rain=[];

for i=1:rand
    X_rain(i)=random ('exp',f_rain);
     RS1_rain(i) =  X_rain(i).*0.84;
     RS2_rain(i) =  X_rain(i).*0.08;
     RS3_rain(i) =  X_rain(i).*0.08;
end

RS1_rain=RS1_rain';
RS2_rain=RS2_rain';
RS3_rain=RS3_rain';

PmRS1_rain=RS1_rain;
PmRS2_rain=RS2_rain;
PmRS3_rain=RS3_rain;

PmRS_rain =[PmRS1_rain PmRS2_rain PmRS3_rain];
```

As it can be seen, this part of the code is similar to the part of the mechanical failure. But in this case, it's considered the division of the three possible release states according to LNE Department, since this part is connected with an OR operator to the seismic failure probability.

5.4.4 Combination of risks

Finally, the last part is about the combination of the risks calculated in the previous sections according to the fault tree scheme adopted. As it can be seen in Figure 5.1, the case of the plant located in Priolo Gargallo expect an AND operator between the seismic failure and the mechanical one in the fault tree, so the aggregation of the two contributions is obtained by a multiplication. The calculation of the top event probability to verify in the case of the tank located in Priolo Gargallo is reported below.

```
PRS1=PeqRS1.*PmRS;
PRS2=PeqRS2.*PmRS;
PRS3=PeqRS3.*PmRS;
P=[PRS1 PRS2 PRS3];
```

While, in the case of the plant located in Porto Marghera, the fault tree scheme expects an OR operator between the seismic failure and the heavy rainfall one, and then an AND operator with the mechanical failure. The calculation of the top event probability in the case of the tank located in Porto Marghera is as follow.

```
PRS1=(PeqRS1+PmRS1_rain).*PmRS;
PRS2=(PeqRS2+PmRS2_rain).*PmRS;
PRS3=(PeqRS3+PmRS3_rain).*PmRS;
P=[PRS1 PRS2 PRS3];
```

In both cases the three contribution of the possible release states are computed in separate equations and then resumed in a vector.
A total number of 10000 simulations were performed with the aim of stochastically taking into account all the potential combinations of probability values.
It’s worth to be noticed that in this Chapter only some parts of the code are shown and that the parameters values displayed are used as example, but they change in the different case studies. The complete code is attached in the Appendix.

Chapter 6

Results presentation

The results obtained in the two case studies highlight how the location of the industrial storage tanks influences the risk: in this Chapter, it's shown how the seismic failure probability distributions are higher in Priolo than in Porto Marghera.
In each location, two calculations are performed: one is the case of the unanchored tank and the other is the case of the anchored tank.

6.1 Mechanical components failure probability

The first result presented is the mechanical components failure probability distribution, since it's the same for each of the case studies, since its deterministic value is taken from the Eni N.A.R. report and it's then converted with an exponential distribution function.
Figure 6.1 shows the mechanical failure probability distribution.

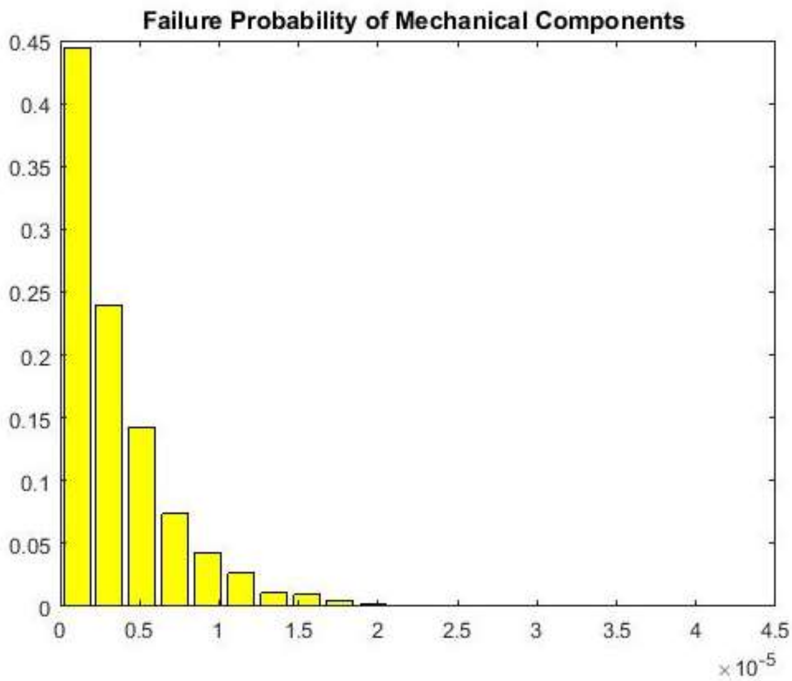

Figure 6.1. *Probability distribution related to mechanical components failure. On the x-axis the values of probability distribution are reported, while on the y-axis the probability of a result to verify.*

As stated in Paragraph 5.4.2, in the case of the mechanical components failure, the division of the LNE Department is not taken into account to avoid the double counting in the top-event probability distribution. Thus, Figure 6.1 illustrates only one probability distribution curve. It's possible to see that release state probability values, concerning only mechanical components failure, are very low, in fact they range from 10^{-5} to 10^{-4}.

6.2 Tank located in Priolo Gargallo

In the first case study, the atmospheric steel tank is located in Priolo Gargallo.

6.2.1 Unanchored tank

Figure 6.2 shows the seismic failure probability distribution of the area for the unanchored tank; green corresponds to earthquake slightly affecting the structure of the tank, thus a negligible loss of containment occurs (RS1), yellow represents a structural damage of the shell, thus giving rise to "slight loss of content" (RS2), while red represent a consistent and rapid loss of content, thus a catastrophic damage of the tank (RS3).

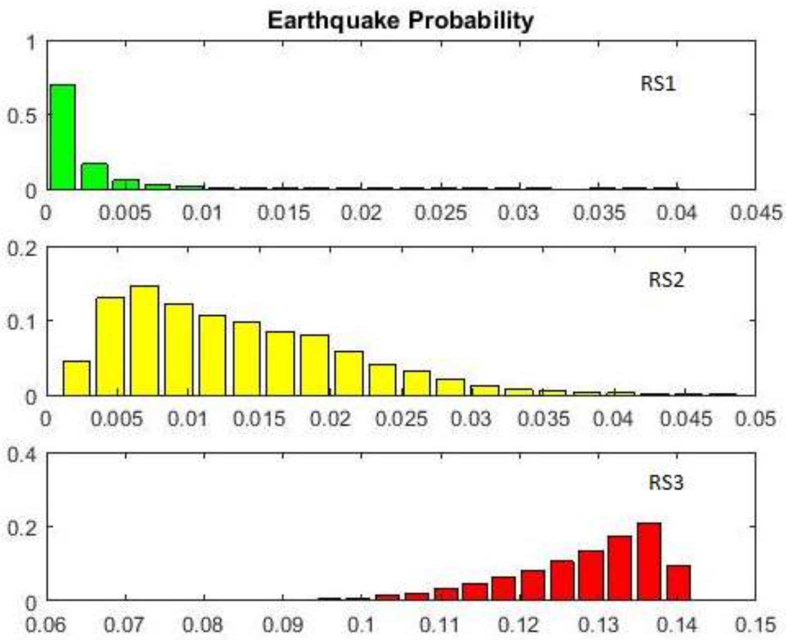

Figure 6.2. *RS1, RS2 and RS3 probability distributions related to failure induced by earthquake scenario occurrences. On the x-axis the values of probability distribution are reported, while on the y-axis the probability of a result to verify.*

With reference to only earthquake-induced failures, quite high release states probability values are observed, ranging from 10^{-3} to 10^{-1}, and the reason is the high seismicity of the area. Looking at Figure 6.2 it's possible to check if the probability of a light damage of the tank is higher than the one of a medium or heavy one. Figure 6.2 highlights that lower probabilities are associated to lower release states (as RS1), whereas higher probability values characterize more critical release states (e.g. RS3).

Finally, Figure 6.3 represents the results obtained from the aggregation of the classical mechanical failures and the damages induced by earthquake occurrence. In this specific case study, it's possible to see how the low values of probability of mechanical failure influence the final probability values, since in the fault tree scheme there's the AND operator that expects the multiplication between the values.

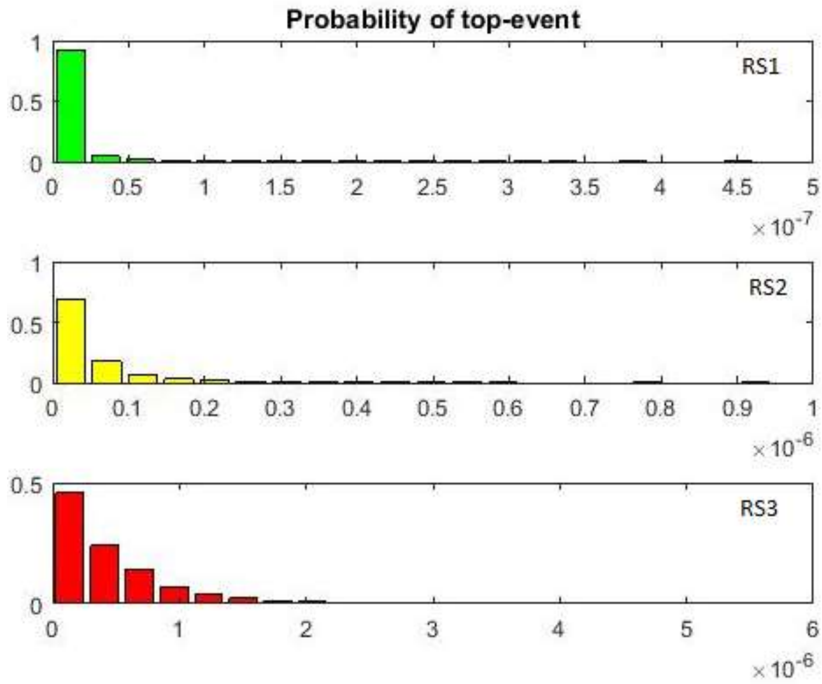

Figure 6.3. *RS1, RS2 and RS3 aggregated probability distributions of top-event occurrence.*

6.2.2 Anchored tank

Figure 6.4 shows the seismic failure probability of the area for the anchored tank; as in the previous case, green expresses the probability of a small damage (RS1), yellow a medium leakage (RS2) and red the rapid total loss of containment (RS3).

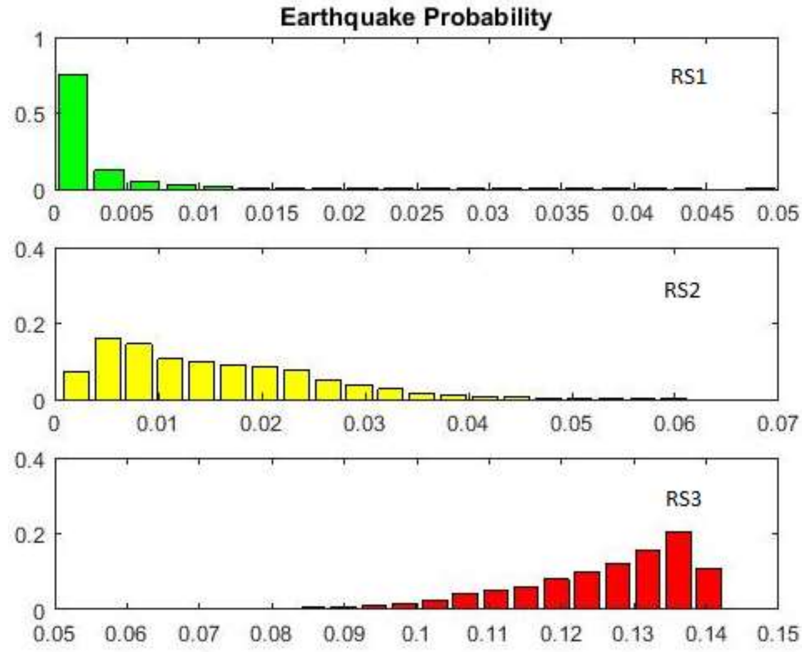

Figure 6.4. *RS1, RS2 and RS3 probability distributions related to failure induced by earthquake scenario occurrences. On the x-axis the values of probability distribution are reported, while on the y-axis the probability of a result to verify.*

Finally, Figure 6.5 represents the results obtained from the aggregation of the classical mechanical failures and the damages induced by earthquake occurrence.

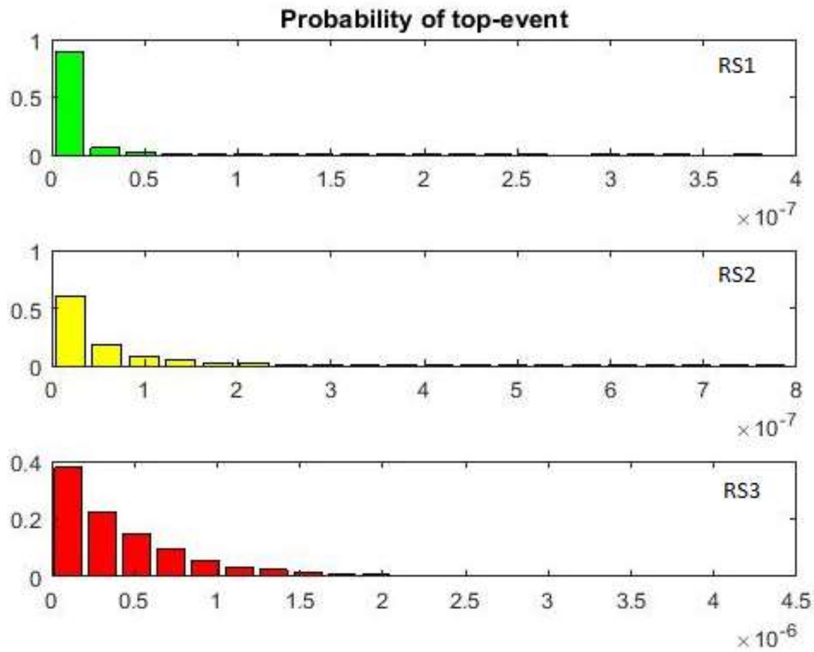

Figure 6.5. *RS1, RS2 and RS3 aggregated probability distributions of top-event occurrence.*

Also in this case, as in the previous one, the low values of probability of mechanical failure influence the final probability values, because of the AND operator in the fault tree scheme.

Now it's possible to compare the results obtained in the case of the unanchored tank with the one of the anchored tank. Before running the simulations in Matlab, the expected result was that the probability of failure due to an earthquake of the anchored tank should have been lower than the one of an unanchored tank. But looking at Figures 6.2 and 6.4 it's possible to see that failure probabilities are very similar in the case of medium damage (RS2) and higher for the catastrophic damage (RS3) in the case of the anchored tank. Concerning this topic, further considerations will be done at the end of the Chapter.

6.3 Tank located in Porto Marghera

The second case study concerns the atmospheric steel tank located in Porto Marghera. In this situation, the calculations relating to the failure probability induced by earthquake scenario occurrence are performed twice: in the case of maximum frequency of return of an earthquake and in case of minimum frequency. These two conditions are represented by Friuli area and Dorsale Ferrarese one, respectively.

6.3.1 Unanchored tank

Figure 6.6a) represents the probability distributions of the different release states related to seismic failure for the unanchored tank in the case of maximum frequency of return of an earthquake.

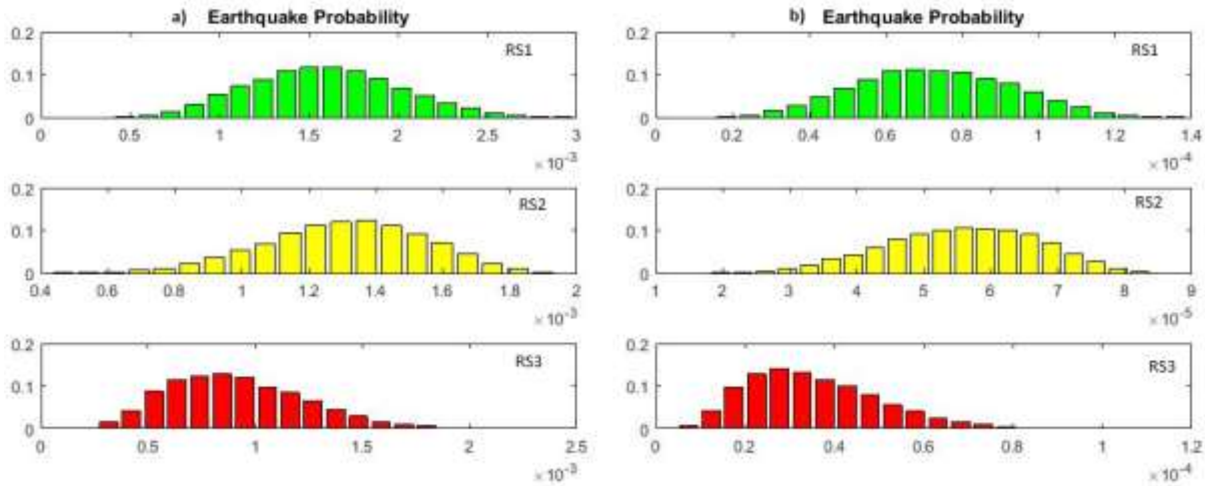

Figure 6.6a) and 6.6b). *RS1, RS2 and RS3 probability distributions related to failure induced by earthquake scenario occurrences. Part a) is calculated with maximum values of the frequency, while part b) with the minimum ones. On the x-axis the values of probability distribution are reported, while on the y-axis the probability of a result to verify.*

On the other hand, Figure 6.6b) represents the probability distributions of the different release states related to seismic failure for the unanchored tank in the case of minimum frequency of return of an earthquake. Comparing Figure 6.6a) and 6.6b), it's possible to see that the two situations differ of one order of magnitude in the case of RS1 andRS3, and even of two orders of magnitude in the case of RS2.

Figure 6.7 shows the probability distributions of the three possible release states in the case of failure induced by heavy rainfall scenario occurrences. Also in the situation of heavy rainfall failure distributions are divided in three levels: green expresses the probability of a small damage (RS1), yellow a medium one (RS2) and red the rapid total loss of containment (RS3).

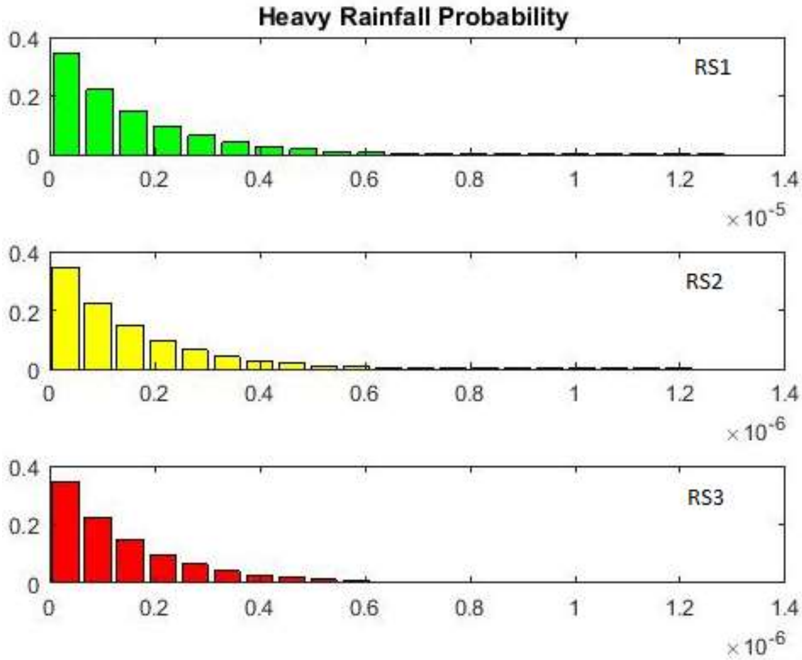

Figure 6.7. *RS1, RS2 and RS3 probability distributions related to failure induced by heavy rainfall scenario occurrences. On the x-axis the values of probability distribution are reported, while on the y-axis the probability of a result to verify.*

Regarding only heavy rainfall-induced failures, low release states probability values are observed (Figure 6.7), ranging from 10^{-6} to 10^{-5}. Higher probability values are related to lower release states whereas lower probabilities are associated to more risky release states.

In Figures 6.8a) and 6.8b) there are the aggregated probability distributions of top-event occurrence, calculated with the maximum and minimum frequency of return of an earthquake respectively. Also in Figures 6.8a) and 6.8b), as in the case of Figures 6.6a) and 6.6b), it's possible to see that comparing the two situations there is an order of magnitude of difference.

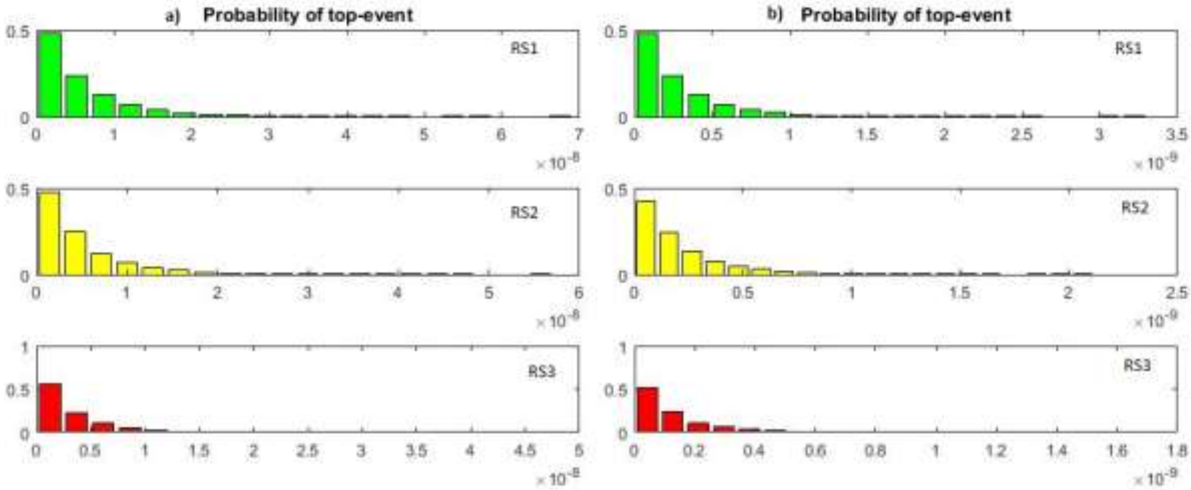

Figure 6.8a) and 6.8b). *RS1, RS2 and RS3 aggregated probability distributions of top-event occurrence. Part a) is calculated with maximum values of the frequency of return of an earthquake, while part b) with the minimum ones.*

6.3.2 Anchored tank

Figure 6.9a) represents the probability distributions of the different release states related to seismic failure for the anchored tank in the case of maximum frequency of return of an earthquake. While Figure 6.9b) represents the probability distributions of the different release states related to seismic failure for the anchored tank in the case of minimum frequency of return of an earthquake.

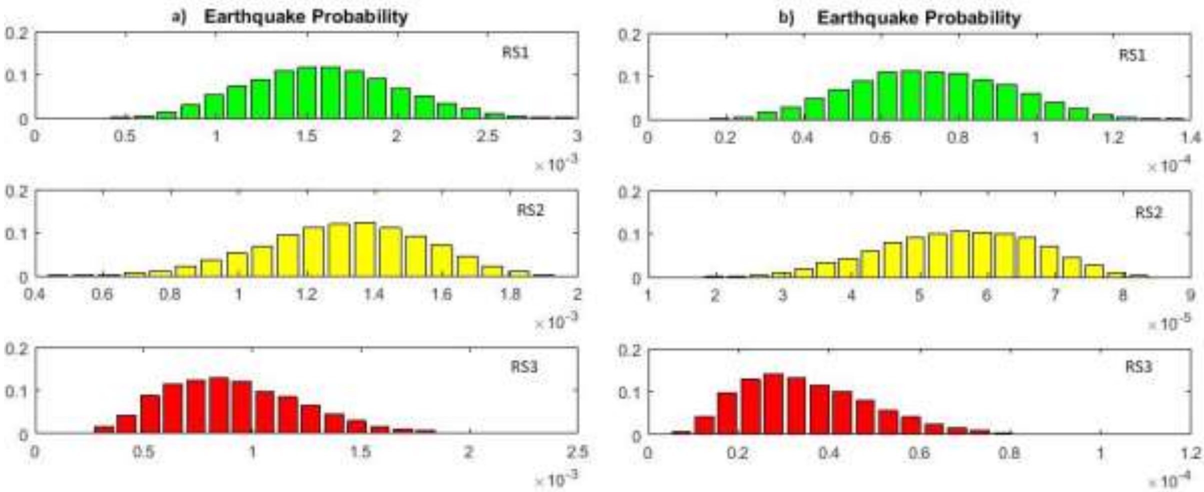

Figure 6.9a) and 6.9b). *RS1, RS2 and RS3 probability distributions related to failure induced by earthquake scenario occurrences. Part a) is calculated with maximum values of the frequency, while part b) with the minimum ones. On the x-axis the values of probability distribution are reported, while on the y-axis the probability of a result to verify.*

It's clear also in this situation that there's an order of magnitude between the case of maximum frequency and the case of minimum frequency.

Figure 6.10 shows the probability distributions of the three possible release states in the case of failure induced by heavy rainfall scenario occurrences.

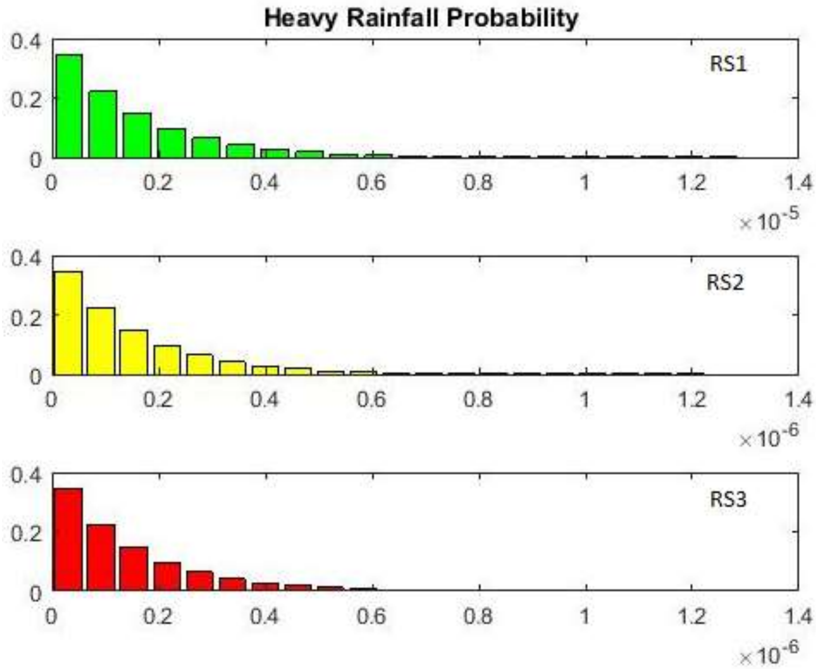

Figure 6.10. *RS1, RS2 and RS3 probability distributions related to failure induced by heavy rainfall scenario occurrences. On the x-axis the values of probability distribution are reported, while on the y-axis the probability of a result to verify.*

As in the case of the unanchored tank, in the case of heavy rainfall-induced failures, low release states probability values are observed (Figure 6.10), ranging from 10^{-6} to 10^{-5}. Higher probability values are related to lower release states whereas lower probabilities are associated to more risky release states.

In Figures 6.11a) and 6.11b) there are the aggregated probabilities of top-event occurrence, calculated with the maximum and minimum frequency of return of an earthquake respectively.

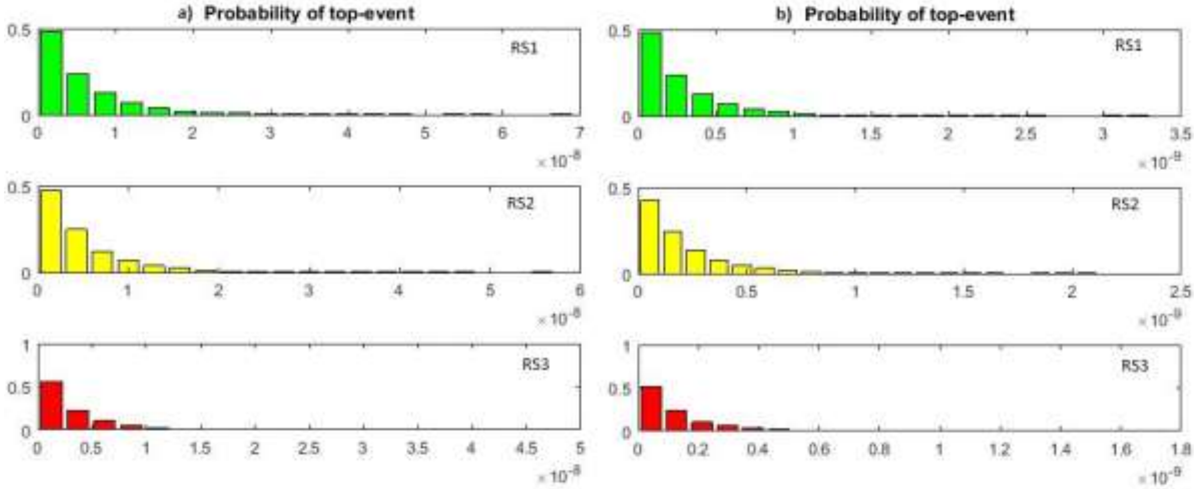

Figure 6.11a) and 6.11b). *RS1, RS2 and RS3 aggregated probabilities of top-event occurrence. Part a) is calculated with maximum values of the frequency of return of an earthquake, while part b) with the minimum ones.*

Conclusions

The aim of this work was to evaluate the risk for an atmospheric steel tank taking into account also natural events.

The first problem that arose was that conventional risk assessment wasn't able to consider also the Na-Tech accidents. For this reason, new techniques were introduced: DyPASI approach and probabilistic fault tree analysis.

The application of DyPASI entails a systematic screening process that, based on early warnings and risk notions, should be able to identify possible Atypical Scenarios available at the time of the analysis. It's composed by several steps and the final result is an updated bow-tie that consider also the Na-Tech.

Once the updated bow-tie was available, the probabilistic fault tree analysis was applied.

The main problem that arose at this point was how to combine deterministic values derived by mechanical risk assessment and probabilistic distribution of earthquakes. The main assumption was to transform mechanical values in a probabilistic way. Since only a value of mechanical failure frequency was present, an exponential distribution function was used. This choice was made because failure frequencies are derived by a structural analysis with a well-established procedure. Years of accidental data collection and innovation gave reliable results. On the other hand, in terms of seismic analysis, data are derived by historical series. These studies analyse all earthquakes with quantitative instrumental data starting only one hundred years ago, so they are based on few events. Their values are more general.

Thanks to this method the risk became a product of single contribution that can be analysed using a Matlab code specially developed.

First of all, it was important to study seismic data of the two locations chosen: Porto Marghera (VE) and Priolo Gargallo (SR). In the first case, it was found that the risk associated to seismic events had a low value; in Priolo the seismic risk is one of the highest of Italy. But Porto Marghera is surrounded by locations that are submitted to a high seismic risk. This fact results in the possibility that also far earthquakes can have consequences on this site. In both locations, simulations are performed for anchored and unanchored tank.

In the case of Porto Marghera, it was considered also the failure probability due to heavy rainfall, as a result of the vulnerability analysis of the area.

The designed code multiplied results of the seismic analysis with the one of the mechanical failure probability in the case of Priolo Gargallo. On the other hand, in the case of Porto Marghera, results of seismic analysis and of rainfall analysis was summed and then the result

was multiplied with the one of mechanical failure probability. A distribution curve of frequencies is obtained. The result expresses the probability of a top-event in each case studies. Differences in the seismic failure probability distributions between Priolo and Porto Marghera are very high and they reflect the dissimilar seismicity of the two areas. In fact, as a result of the vulnerability analysis of the two locations it's evident that Priolo is a highly seismic area and on the other hand, Porto Marghera is not.
Comparing the cases of the unanchored tank with those of the anchored tank, the expected results are not confirmed; conversely, they highlight that failure probabilities are higher in the case of the anchored tank. Thus, in future studies, it's better to consider seismic insulation systems, as the one shown in Figure below, at least in seismic zones.

Figure. *Example of seismic insulation system.*

Results have highlighted how taking into account earthquake occurrence is a crucial step in defining release occurrence probabilities in areas prone to seismic hazard.
When dealing with seismic risk, a probabilistic approach might thus be preferred due to significant uncertainties that are involved in the analysis.
In this thesis, it's used a method to extend probabilistic approaches also to the classic QRA analysis with the aim to formalize a probabilistic fault tree analysis to be performed when seismic risk has to be faced. In this way, a combination of natural risk and chemical one is possible.

Appendix

Matlab codes

A. Unanchored tank in Priolo Gargallo

```
rand=input('number of iterations')


% Earthquake

R=xlsread('DistribuzioniPriolo.xlsx', 'distanza', 'A1:A8');
M=xlsread('DistribuzioniPriolo.xlsx', 'Magnitudo', 'A1:H1');
MP=xlsread('DistribuzioniPriolo.xlsx', 'matrice', 'A1:H8');
F=xlsread('DistribuzioniPriolo.xlsx', 'Frequenza', 'A1:H1');

r=length(R);
m=length(M);
logPGA=[];
for i=1:r
    for j=1:m
        logPGA(i,j)=1.344+0.328*M(j)-1.09*log10(sqrt(R(i)^2+5^2))+0.096;
    end
end

sigma=0.32; % Shape value of LogPGA
mu2=0.15; % Mean value of Fragility Medium hole
sigma2=0.7; % shape value of Fragility Medium hole
mu3=1.06; % Mean value of Fragility large hole
sigma3=0.8;  % Shape value of Fragility large hole
PeqRS1=[];
PeqRS2=[];
PeqRS3=[];
PeqRS1=zeros(rand,1);
PeqRS2=zeros(rand,1);
PeqRS3=zeros(rand,1);

for i=1:rand
%     PGA1=10.^(logPGA+sigma);
    PGA1=random ('norm',logPGA,sigma);
    PGA=(10.^PGA1)*9.81/100;
    RS3eq= cdf('logn',PGA,mu3,sigma3);
    RS2eq=cdf('logn',PGA,mu2,sigma2);
    Prs1=(1-RS2eq).*(MP./100);
    Prs2=(RS2eq-RS3eq).*(MP./100);
    Prs3=RS3eq.*(MP./100);
    PfRS11=sum(Prs1).*F;
    PfRS1=sum(PfRS11(:));
    PfRS22=sum(Prs2).*F;
```

```
    PfRS2=sum(PfRS22(:));
    PfRS33=sum(Prs3).*F;
    PfRS3=sum(PfRS33(:));
    PeqRS1(i)=[PfRS1 ];
    PeqRS2(i)=[PfRS2 ];
    PeqRS3(i)=[PfRS3 ];
    i=i+1;
end

PeqRS =[PeqRS1 PeqRS2 PeqRS3];
meaneq=mean(PeqRS);


[countsa,centersa] = hist(PeqRS1,20);
[countsb,centersb] = hist(PeqRS2,20);
[countsc,centersc] = hist(PeqRS3,20);
[countspga,centerspga] = hist(PGA1,20);

ya=linspace(0,(max(countsa/rand)+0.05));
yb=linspace(0,(max(countsb/rand)+0.05));
yc=linspace(0,(max(countsc/rand)+0.05));


figure (1)
bar(centerspga,(countspga/rand),'g');


figure (2)
subplot(3,1,1)
bar(centersa,(countsa/rand),'g');
title ('Earthquake Probability')
% axis([0 0.25 0 inf])

subplot(3,1,2)
bar(centersb,(countsb/rand),'y')
% axis([0 0.25 0 inf])

subplot(3,1,3)
bar(centersc,(countsc/rand),'r')
% axis([0 0.25 0 inf])


% Failure rate of mechanical components

lambda=3.573E-6; %event/years
time=50; %years
t=[0:0.1:time];
f=lambda*exp(-lambda.*time);
X=[];
for i=1:rand
    X(i)=random ('exp',f);
    RS(i)=X(i);
end
RS=RS';

PmRS=RS;
```

```
[countsd,centersd] = hist(PmRS,20);

yd=linspace(0,(max(countsd/rand)+0.05),100);

figure (3)
% subplot(3,1,1)
bar(centersd,(countsd/rand),'y');
title ('Failure Probability of Mechanical Components ')

% Probability of release from atmospheric tank

PRS1=PeqRS1.*PmRS;
PRS2=PeqRS2.*PmRS;
PRS3=PeqRS3.*PmRS;
P=[PRS1 PRS2 PRS3];
meanP=mean(P);

[counts1,centers1] = hist(PRS1,20);
[counts2,centers2] = hist(PRS2,20);
[counts3,centers3] = hist(PRS3,20);

y1=linspace(0,(max(counts1/rand)+0.05),100);
y2=linspace(0,(max(counts2/rand)+0.05),100);
y3=linspace(0,(max(counts3/rand)+0.05),100);

figure (4)

subplot(3,1,1)
bar(centers1,(counts1/rand),'g')
title ('Probability of top-event')
subplot(3,1,2)
bar(centers2,(counts2/rand),'y')
subplot(3,1,3)
bar(centers3,(counts3/rand),'r')
```

B. Anchored tank in Priolo Gargallo

```
rand=input('number of iterations')


% Earthquake

R=xlsread('DistribuzioniPriolo.xlsx', 'distanza', 'A1:A8');
M=xlsread('DistribuzioniPriolo.xlsx', 'Magnitudo', 'A1:H1');
MP=xlsread('DistribuzioniPriolo.xlsx', 'matrice', 'A1:H8');
F=xlsread('DistribuzioniPriolo.xlsx', 'Frequenza', 'A1:H1');

r=length(R);
m=length(M);
logPGA=[];
for i=1:r
    for j=1:m
        logPGA(i,j)=1.344+0.328*M(j)-1.09*log10(sqrt(R(i)^2+5^2))+0.096;
    end
end
```

```
sigma=0.32; % % Shape value of LogPGA
mu2=0.3; % Mean value of Fragility Medium hole
sigma2=0.6; % shape value of Fragility Medium hole
mu3=1.25; % Mean value of Fragility large hole
sigma3=0.65;  % Shape value of Fragility large hole
PeqRS1=[];
PeqRS2=[];
PeqRS3=[];
PeqRS1=zeros(rand,1);
PeqRS2=zeros(rand,1);
PeqRS3=zeros(rand,1);

for i=1:rand
%     PGA1=10.^(logPGA+sigma);
    PGA1=random ('norm',logPGA,sigma);
    PGA=(10.^PGA1)*9.81/100;
    RS3eq= cdf('logn',PGA,mu3,sigma3);
    RS2eq=cdf('logn',PGA,mu2,sigma2);
    Prs1=(1-RS2eq).*(MP./100);
    Prs2=(RS2eq-RS3eq).*(MP./100);
    Prs3=RS3eq.*(MP./100);
    PfRS11=sum(Prs1).*F;
    PfRS1=sum(PfRS11(:));
    PfRS22=sum(Prs2).*F;
    PfRS2=sum(PfRS22(:));
    PfRS33=sum(Prs3).*F;
    PfRS3=sum(PfRS33(:));
    PeqRS1(i)=[PfRS1 ];
    PeqRS2(i)=[PfRS2 ];
    PeqRS3(i)=[PfRS3 ];
    i=i+1;
end

PeqRS =[PeqRS1 PeqRS2 PeqRS3];
meaneq=mean(PeqRS);

[countsa,centersa] = hist(PeqRS1,20);
[countsb,centersb] = hist(PeqRS2,20);
[countsc,centersc] = hist(PeqRS3,20);
[countspga,centerspga] = hist(PGA1,20);

ya=linspace(0,(max(countsa/rand)+0.05));
yb=linspace(0,(max(countsb/rand)+0.05));
yc=linspace(0,(max(countsc/rand)+0.05));


figure (1)
bar(centerspga,(countspga/rand),'g');


figure (2)
subplot(3,1,1)
bar(centersa,(countsa/rand),'g');
title ('Earthquake Probability')
% axis([0 0.25 0 inf])

subplot(3,1,2)
bar(centersb,(countsb/rand),'y')
```

```
% axis([0 0.25 0 inf])

subplot(3,1,3)
bar(centersc,(countsc/rand),'r')
% axis([0 0.25 0 inf])


% Failure rate of mechanical components

lambda=3.573E-6; %event/years
time=50; %years
t=[0:0.1:time];
f=lambda*exp(-lambda.*time);
X=[];
for i=1:rand
    X(i)=random ('exp',f);
    RS(i)=X(i);
end
RS=RS';

PmRS=RS;

[countsd,centersd] = hist(PmRS,20);

yd=linspace(0,(max(countsd/rand)+0.05),100);

figure (3)
% subplot(3,1,1)
bar(centersd,(countsd/rand),'y');
title ('Failure Probability of Mechanical Components ')


% Probability of release from atmospheric tank

PRS1=PeqRS1.*PmRS;
PRS2=PeqRS2.*PmRS;
PRS3=PeqRS3.*PmRS;
P=[PRS1 PRS2 PRS3];
meanP=mean(P);

[counts1,centers1] = hist(PRS1,20);
[counts2,centers2] = hist(PRS2,20);
[counts3,centers3] = hist(PRS3,20);

y1=linspace(0,(max(counts1/rand)+0.05),100);
y2=linspace(0,(max(counts2/rand)+0.05),100);
y3=linspace(0,(max(counts3/rand)+0.05),100);

figure (4)

subplot(3,1,1)
bar(centers1,(counts1/rand),'g')
title ('Probability of top-event')
subplot(3,1,2)
bar(centers2,(counts2/rand),'y')
subplot(3,1,3)
bar(centers3,(counts3/rand),'r')
```

C. Unanchored tank in Porto Marghera

```
rand=input('number of iterations')


% Earthquake

R=xlsread('DistribuzioniPortoMarghera.xlsx', 'distanza', 'A1:A14');
M=xlsread('DistribuzioniPortoMarghera.xlsx', 'Magnitudo', 'A1:F1');
MP=xlsread('DistribuzioniPortoMarghera.xlsx', 'matrice', 'A1:F14');
F=xlsread('DistribuzioniPortoMarghera.xlsx', 'Frequenza', 'A1:F1');

r=length(R);
m=length(M);
logPGA=[];
for i=1:r
    for j=1:m
        logPGA(i,j)=1.344+0.328*M(j)-1.09*log10(sqrt(R(i)^2+5^2))+0.096;
    end
end

sigma=0.32; % Shape value of LogPGA
mu2=0.15; % Mean value of Fragility Medium hole
sigma2=0.7; % shape value of Fragility Medium hole
mu3=1.06; % Mean value of Fragility large hole
sigma3=0.8;  % Shape value of Fragility large hole
PeqRS1=[];
PeqRS2=[];
PeqRS3=[];
PeqRS1=zeros(rand,1);
PeqRS2=zeros(rand,1);
PeqRS3=zeros(rand,1);

for i=1:rand
%     PGA1=10.^(logPGA+sigma);
    PGA1=random ('norm',logPGA,sigma);
    PGA=(10.^PGA1).*9.81/100;
    RS3eq= cdf('logn',PGA,mu3,sigma3);
    RS2eq=cdf('logn',PGA,mu2,sigma2);
    Prs1=(1-RS2eq).*(MP./100);
    Prs2=(RS2eq-RS3eq).*(MP./100);
    Prs3=RS3eq.*(MP./100);
    PfRS11=sum(Prs1).*F;
    PfRS1=sum(PfRS11(:));
    PfRS22=sum(Prs2).*F;
    PfRS2=sum(PfRS22(:));
    PfRS33=sum(Prs3).*F;
    PfRS3=sum(PfRS33(:));
    PeqRS1(i)=[PfRS1 ];
    PeqRS2(i)=[PfRS2 ];
    PeqRS3(i)=[PfRS3 ];
    i=i+1;
end

PeqRS =[PeqRS1 PeqRS2 PeqRS3];
meaneq=mean(PeqRS);


[countsa,centersa] = hist(PeqRS1,20);
```

```
[countsb,centersb] = hist(PeqRS2,20);
[countsc,centersc] = hist(PeqRS3,20);
[countspga,centerspga] = hist(PGA1,20);

ya=linspace(0,(max(countsa/rand)+0.05));
yb=linspace(0,(max(countsb/rand)+0.05));
yc=linspace(0,(max(countsc/rand)+0.05));


figure (1)
bar(centerspga,(countspga/rand),'g');


figure (2)
subplot(3,1,1)
bar(centersa,(countsa/rand),'g');
title ('Earthquake Probability')
% axis([0 0.25 0 inf])

subplot(3,1,2)
bar(centersb,(countsb/rand),'y')
% axis([0 0.25 0 inf])

subplot(3,1,3)
bar(centersc,(countsc/rand),'r')
% 1axis([0 0.25 0 inf])


% Failure rate of mechanical components

lambda=3.573E-6; %event/years
time=50; %years
t=[0:0.1:time];
f=lambda*exp(-lambda.*time);
X=[];
for i=1:rand
    X(i)=random ('exp',f);
     RS(i) = X(i);

end
RS=RS';


PmRS=RS;

[countsd,centersd] = hist(PmRS,20);

yd=linspace(0,(max(countsd/rand)+0.05),100);

figure (3)

% subplot(3,1,1)
bar(centersd,(countsd/rand),'y');
title ('Failure Probability of Mechanical Components ')
```

```
% Heavy rainfall

lambda_rain=4/17; %event/years
time=50; %years
f_rain=lambda_rain*exp(-lambda_rain.*time);
X_rain=[];
for i=1:rand
    X_rain(i)=random ('exp',f_rain);
     RS1_rain(i) =  X_rain(i).*0.84;
     RS2_rain(i) =  X_rain(i).*0.08;
     RS3_rain(i) =  X_rain(i).*0.08;
end
RS1_rain=RS1_rain';
RS2_rain=RS2_rain';
RS3_rain=RS3_rain';

PmRS1_rain=RS1_rain;
PmRS2_rain=RS2_rain;
PmRS3_rain=RS3_rain;

PmRS_rain =[PmRS1_rain PmRS2_rain PmRS3_rain];
meanm_rain=mean(PmRS_rain);

[countsd_rain,centersd_rain] = hist(PmRS1_rain,20);
[countse_rain,centerse_rain] = hist(PmRS2_rain,20);
[countsf_rain,centersf_rain] = hist(PmRS3_rain,20);

yd_rain=linspace(0,(max(countsd_rain/rand)+0.05),100);
ye_rain=linspace(0,(max(countse_rain/rand)+0.05),100);
yf_rain=linspace(0,(max(countsf_rain/rand)+0.05),100);

figure (4)

subplot(3,1,1)
bar(centersd_rain,(countsd_rain/rand),'g');
title ('Heavy Rainfall Probability ')
subplot(3,1,2)
bar(centerse_rain,(countse_rain/rand),'y')
subplot(3,1,3)
bar(centersf_rain,(countsf_rain/rand),'r')

% Probability of release from atmospheric tank

PRS1=(PeqRS1+PmRS1_rain).*PmRS;
PRS2=(PeqRS2+PmRS2_rain).*PmRS;
PRS3=(PeqRS3+PmRS3_rain).*PmRS;
P=[PRS1 PRS2 PRS3];
meanP=mean(P);

[counts1,centers1] = hist(PRS1,20);
[counts2,centers2] = hist(PRS2,20);
[counts3,centers3] = hist(PRS3,20);

y1=linspace(0,(max(counts1/rand)+0.05),100);
y2=linspace(0,(max(counts2/rand)+0.05),100);
y3=linspace(0,(max(counts3/rand)+0.05),100);

figure (5)
```

```
subplot(3,1,1)
bar(centers1,(counts1/rand),'g')
title ('Probability of top-event')

subplot(3,1,2)
bar(centers2,(counts2/rand),'y')

subplot(3,1,3)
bar(centers3,(counts3/rand),'r')
```

D. Anchored tank in Porto Marghera

```
rand=input('number of iterations')


% Earthquake

R=xlsread('DistribuzioniPortoMarghera.xlsx', 'distanza', 'A1:A14');
M=xlsread('DistribuzioniPortoMarghera.xlsx', 'Magnitudo', 'A1:F1');
MP=xlsread('DistribuzioniPortoMarghera.xlsx', 'matrice', 'A1:F14');
F=xlsread('DistribuzioniPortoMarghera.xlsx', 'Frequenza', 'A1:F1');

r=length(R);
m=length(M);
logPGA=[];
for i=1:r
    for j=1:m
        logPGA(i,j)=1.344+0.328*M(j)-1.09*log10(sqrt(R(i)^2+5^2))+0.096;
    end
end

sigma=0.32; % Shape value of LogPGA
mu2=0.3; % Mean value of Fragility Medium hole
sigma2=0.6; % shape value of Fragility Medium hole
mu3=1.25; % Mean value of Fragility large hole
sigma3=0.65;  % Shape value of Fragility large hole
PeqRS1=[];
PeqRS2=[];
PeqRS3=[];
PeqRS1=zeros(rand,1);
PeqRS2=zeros(rand,1);
PeqRS3=zeros(rand,1);

for i=1:rand
%     PGA1=10.^(logPGA+sigma);
    PGA1=random ('norm',logPGA,sigma);
    PGA=(10.^PGA1).*9.81/100;
    RS3eq= cdf('logn',PGA,mu3,sigma3);
    RS2eq=cdf('logn',PGA,mu2,sigma2);
    Prs1=(1-RS2eq).*(MP./100);
    Prs2=(RS2eq-RS3eq).*(MP./100);
    Prs3=RS3eq.*(MP./100);
    PfRS11=sum(Prs1).*F;
    PfRS1=sum(PfRS11(:));
```

```
    PfRS22=sum(Prs2).*F;
    PfRS2=sum(PfRS22(:));
    PfRS33=sum(Prs3).*F;
    PfRS3=sum(PfRS33(:));
    PeqRS1(i)=[PfRS1 ];
    PeqRS2(i)=[PfRS2 ];
    PeqRS3(i)=[PfRS3 ];
    i=i+1;
end

PeqRS =[PeqRS1 PeqRS2 PeqRS3];
meaneq=mean(PeqRS);


[countsa,centersa] = hist(PeqRS1,20);
[countsb,centersb] = hist(PeqRS2,20);
[countsc,centersc] = hist(PeqRS3,20);
[countspga,centerspga] = hist(PGA1,20);

ya=linspace(0,(max(countsa/rand)+0.05));
yb=linspace(0,(max(countsb/rand)+0.05));
yc=linspace(0,(max(countsc/rand)+0.05));


figure (1)
bar(centerspga,(countspga/rand),'g');


figure (2)
subplot(3,1,1)
bar(centersa,(countsa/rand),'g');
title ('Earthquake Probability')

subplot(3,1,2)
bar(centersb,(countsb/rand),'y')

subplot(3,1,3)
bar(centersc,(countsc/rand),'r')


% Failure rate of mechanical components

lambda=3.573E-6; %event/years
time=50; %years
t=[0:0.1:time];
f=lambda*exp(-lambda.*time);
X=[];
for i=1:rand
    X(i)=random ('exp',f);
     RS(i) = X(i);

end
RS=RS';

PmRS=RS;
[countsd,centersd] = hist(PmRS,20);
```

```
yd=linspace(0,(max(countsd/rand)+0.05),100);

figure (3)

% subplot(3,1,1)
bar(centersd,(countsd/rand),'y');
title ('Failure Probability of Mechanical Components ')


% Heavy rainfall

lambda_rain=4/17; %event/years
time=50; %years
f_rain=lambda_rain*exp(-lambda_rain.*time);

X_rain=[];
for i=1:rand
    X_rain(i)=random ('exp',f_rain);
     RS1_rain(i) =  X_rain(i).*0.84;
     RS2_rain(i) =  X_rain(i).*0.08;
     RS3_rain(i) =  X_rain(i).*0.08;
end
RS1_rain=RS1_rain';
RS2_rain=RS2_rain';
RS3_rain=RS3_rain';

PmRS1_rain=RS1_rain;
PmRS2_rain=RS2_rain;
PmRS3_rain=RS3_rain;

PmRS_rain =[PmRS1_rain PmRS2_rain PmRS3_rain];
meanm_rain=mean(PmRS_rain);

[countsd_rain,centersd_rain] = hist(PmRS1_rain,20);
[countse_rain,centerse_rain] = hist(PmRS2_rain,20);
[countsf_rain,centersf_rain] = hist(PmRS3_rain,20);

yd_rain=linspace(0,(max(countsd_rain/rand)+0.05),100);
ye_rain=linspace(0,(max(countse_rain/rand)+0.05),100);
yf_rain=linspace(0,(max(countsf_rain/rand)+0.05),100);

figure (4)

subplot(3,1,1)
bar(centersd_rain,(countsd_rain/rand),'g');
title ('Heavy Rainfall Probability ')
subplot(3,1,2)
bar(centerse_rain,(countse_rain/rand),'y')
subplot(3,1,3)
bar(centersf_rain,(countsf_rain/rand),'r')


% Probability of release from atmospheric tank


PRS1=(PeqRS1+PmRS1_rain).*PmRS;
PRS2=(PeqRS2+PmRS2_rain).*PmRS;
```

```
PRS3=(PeqRS3+PmRS3_rain).*PmRS;
P=[PRS1 PRS2 PRS3];
meanP=mean(P);

[counts1,centers1] = hist(PRS1,20);
[counts2,centers2] = hist(PRS2,20);
[counts3,centers3] = hist(PRS3,20);

y1=linspace(0,(max(counts1/rand)+0.05),100);
y2=linspace(0,(max(counts2/rand)+0.05),100);
y3=linspace(0,(max(counts3/rand)+0.05),100);

figure (5)

subplot(3,1,1)
bar(centers1,(counts1/rand),'g')
title ('Probability of top-event')

subplot(3,1,2)
bar(centers2,(counts2/rand),'y')

subplot(3,1,3)
bar(centers3,(counts3/rand),'r')
```

References

Antonioni G., Bonvicini S., Spadoni G. and Cozzani V. (2009). Development of a framework for the risk assessment of Na-Tech accidental events. *Reliability Engineering and System Safety*, **94**, 1442-1450.

Bindi D., Luzi L., Pacor F., Sabetta F. and Massa M. (2009). Towards a new reference ground motion prediction equation for Italy: update of the Sabetta-Pugliese (1996). *Bull Earthquake Eng,* **7**, 591-608.

Campedel M., Cozzani V., Krausmann E. and Cruz A. M. (2008). Analysis of Natech Accidents recorded in Major Accident Databases. In: *Ninth International Probabilistic Safety Assessment and Management Conference (Hong Kong, China).*

Cruz A. M., Steinberg L. J., Vetere Arellano A. L., Nordvik J. P. and Pisano F. in the European Commission (2004). *State of the Art in Natech Risk Management.*

Di Carluccio A. (2007). Structural Characterisation and Seismic Evaluation of Steel Equipments in Industrial Plants. *PhD Thesis in Seismic Risk*, Polo delle Scienze e delle Tecnologie, University of Napoli (Federico II).

Eni N.A.R. Report (2013). Analisi di Sicurezza a supporto della dichiarazione di Non Aggravio di Rischio.

European Parliament (2012). *Directive 2012/18/UE.*

Gnesotto A. (2016). Risk analysis in atmospheric and pressurized tank subjected to seismic effects. *Master Thesis in Chemical and Process Engineering*, DII, University of Padova.

Jain P., Pasman H. J., Waldram S. P., Rogers W. J. and Mannan M. S. (2016). Did we learn about risk control since Seveso? Yes, we surely did, but is it enough? An historical brief and problem analysis. *Journal of Loss Prevention in the Process Industries*.

Necci Amos (2015). Cascading events triggering industrial accidents: quantitative assessment of natech and domino scenarios. *PhD Thesis in Environmental and Safety chemical engineering*, DIPIC, University of Bologna.

Paltrinieri N., Tugnoli A., Buston J., Wardman M. and Cozzani V. (2013). DyPASI: from Information Retrieval to Integration of HAZID Process. *Chemical Engineering Transactions*, **32**, 433-438.

Paltrinieri N., Tugnoli A., Buston J., Wardman M. and Cozzani V. (2013). Dynamic Procedure for Atypical Scenarios Identification (DyPASI): A new systematic HAZID tool. *Journal of Loss Prevention in the Process Industries*, **26**, 683-695.

Salzano E., Agreda A. G., Di Carluccio A. and Fabbrocino G. (2009). Risk assessment and early warning systems for industrial facilities in seismic zones. *Reliability Engineering and System Safety*, **94**, 1577-1584.

Salzano E., Iervolino I. and Fabbrocino G. (2003). Seismic risk of atmospheric storage tanks in the framework of quantitative risk analysis. *Journal of Loss Prevention in the process industries*, **16**, 403-409.

Schüller J. C. H., Brinkman J.L., Van Gestel P.J. and van Otterloo R.W. (1997). *Methods for determining and processing probabilities, "Red Book"* (2th ed.).

Sinnott R. and Towler G. (2009). *Chemical Engineering Design* (5th ed.). Butterworth-Heinemann, Oxford (UK).

Veneto regional council (2012). Eventi Meteorologici Estremi – Dati e valutazioni sulla radicalizzazione del clima in Veneto.

Vianello C., Zanini M. A. and Maschio G. (2016). Probabilistic Fault Tree Analysis of Refinery Plant Components subjects to Earthquake Scenarios. *Chemical Engineering Transaction*, **52**.

<u>Web-sites</u>

`http://enatech.jrc.ec.europa.eu/` (last access 19/12/16)

`http://www.ingv.it/it/` (last access 31/03/2017)

`http://www.protezionecivile.gov.it/jcms/it/cen_vulc_rischio.wp` (last access 31/03/2017)

`http://www.sozogaku.com/fkd/en/` (last access 31/03/2017)

`http://www.aria.developpement-durable.gouv.fr/find-accident/?lang=en` (last access 31/03/2017)

`https://www.mepa.org.mt/topics-seveso-background` (last access 7/11/2016)

`http://ec.europa.eu/environment/seveso/legislation.htm` (last access 7/11/2016)